

**A comparison of the effect of curcumin
treatment on apoptosis, necrosis and
autophagy in a MCF-7 mammary
adenocarcinoma and a MCF-12A healthy
mammary epithelial cell line**

Martine van den Heever

*Dissertation presented for the degree of Master of Physiological
Sciences*



Stellenbosch University

Department of Physiological Sciences

Faculty of natural Sciences

Promoter: Anna-Mart Engelbrecht

Co-Promoter: Benjamin Loos

March 2009

Declaration

By submitting this dissertation electronically, I declare that the entirety of the work contained therein is my own, original work, that I am the owner of the copyright thereof (unless to the extent explicitly otherwise stated) and that I have not previously in its entirety or in part submitted it for obtaining any qualification.

Date: 20 February 2009

Copyright © 2008 Stellenbosch University

All rights reserved

Abstract

Breast cancer is currently the primary cause of cancer-related death in women worldwide. Conventional treatments such as radiation and chemotherapy have many deleterious and long lasting side-effects, some of which are permanent, such as infertility. As certain tumour cells can also acquire resistance to chemotherapy, the need for the development of a less severe, yet more effective, targeted anti-cancer treatment exists. Curcumin, a plant polyphenol from *Curcuma longa*, has long been thought to possess antitumour, antioxidant, anti-arthritic, anti-amyloid, anti-ischemic and anti-inflammatory properties. Numerous studies conducted over the past sixty years confirm this. We aimed at examining the effect of curcumin on cell viability and the different modes of cell death, namely apoptosis, necrosis and autophagy, in the MCF-12A (non-tumorigenic mammary epithelial) and MCF-7 (mammary adenocarcinoma) cell lines.

Cells were incubated with different doses of curcumin to evaluate the dose response through a MTT assay. Thereafter, cells were incubated with 200 μ M curcumin for 48 hrs and stained with markers and DNA stains for apoptosis (Hoechst, Caspase-3, PARP), necrosis (Propidium Iodide) and autophagy (LC3B and Beclin-1). Cells were examined via fluorescence microscopy, Western Blot- and FACS analyses. MTT results showed no significant decrease in viability in the MCF-12A cell line after curcumin treatment. However, a significant decrease in viability was observed in MCF-7 cells after treatment with 200 μ M curcumin ($p < 0.05$). Treated MCF-7 cells also show clear LC3B expression. FACS results show a significant difference in Hoechst mean fluorescence intensity in MCF-7 cells after curcumin treatment ($p < 0.05$). This study provides evidence that MCF-7 cells respond to a 200 μ M dose of

curcumin treatment through metabolic change and induction of the autophagic pathway. The model system used in this study provides groundwork for further cell culture based studies regarding breast cancer and curcumin.

Opsomming

Borskanker is tans wêreldwyd die hooforsaak van kankerverwante sterftes onder vroue. Konvensionele behandeling soos bestraling en chemoterapie het verskeie en ook blywende nuwe-effekte, soos byvoorbeeld onvrugbaarheid. Aangesien sekere tumorselle ook weerstand teen chemoterapeutiese middels kan ontwikkel, bestaan 'n behoefte aan die ontwikkeling van 'n minder skadelike, dog meer effektiewe, geteikende antikanker behandeling. Curcumin is 'n plant polifenol afkomstig van *Curcuma longa*, wat beweerlik antitumor, antioksidant, anti-aritmiese, anti-ameloiëde, anti-iskemiese, en anti-inflammatoriese eienskappe besit. Verskeie studies wat in die afgelope 60 jaar gedoen is, bevestig dit. Ons mikpunt was om die effek van curcumin op sellewensvatbaarheid en die verskillende modusse van seldood, naamlik apoptose, nekrose, en outofagie in die MCF-12A (nie-tumorigeniese borsepiteel) en MCF-7 (mamma-adenokarsinoom) sellyne, te ondersoek. Selle is met verskillende dosisse curcumin behandel om sodoende die dosisrespons via 'n MTT essai te evalueer. Daarna is selle vir 'n tydperk van 48 h met 200 µM curcumin geïnkubeer, en met fluorochroom-gekoppelde merkers en DNA kleurmiddels vir apoptose (Hoechst, Caspase-3 en PARP), nekrose (PI) en outofagie (LC3B en Beclin), gekleur. Selle is via fluoresensie mikroskopie, Western klad en vloesitometrie tegnieke ondersoek. MTT resultate het geen betekenisvolle afname in lewensvatbaarheid in MCF-12 selle tot gevolg gehad nie, terwyl dit wel 'n betekenisvolle afname in lewensvatbaarheid in MCF-7 selle, na behandeling met 200 µM curcumin, teweeg gebring het ($p < 0.05$). Fluoresensie mikroskoopbeelde toon duidelike uitdrukking van LC3B in MCF-7 selle na 48 h inkubasie met 200 µM curcumin, wat op die induksie van die outofagie padweg dui. Vloesitometrie resultate

toon ook 'n verskil in Hoechst gemiddelde fluoresensie intensiteit, 'n merker vir apoptose, in MCF-7 selle na curcumin behandeling ($p < 0.05$). Die betrokke studie verskaf bewyse dat die MCF-7 sellyn deur middel van metaboliese verandering en induksie van die outofagie pad op 'n 200 μM dosis curcumin reageer. Die modelsisteem wat in hierdie studie gebruik is, lê die grondslag vir verdere selkultuur gebaseerde studies aangaande borskanker en curcumin.

Acknowledgements

I would like to express my sincerest thanks towards the following persons:

My supervisor, Dr Anna-Mart Engelbrecht, one of the very few people I know who will truly do everything in her power to help another. Thank you for your constant support and understanding.

My co-supervisor, Benjamin Loos, who, in spite of his busy schedule, has never been too busy to help me.

My parents and sister, who make everything in life easier.

Mark Thomas and Jamie Imbriolo, for help with Western Blots.

Dr Rob Smith, for valuable technical advice.

Dr Theo Nell, for help with editing.

List of Abbreviations

Units of measurement

%	Percent
µg	Microgram
µl	Microlitre
µm	Micrometer
µM	Micromolar
g	Gram
hrs	Hours
kDa	Kilodalton
l/L	Litre
M	Molar
mg	Milligram
min	Minute
ml	millilitre
°C	Degrees Celcius
U	units

General

3-D	Three-dimensional
Ab	Antibody
AIF	Apoptosis-inducing Factor
ANOVA	Analysis of variance
AP	Activated Protein

APS	Ammonium Persulfate
ATP	Adenosine Triphosphate
BSA	Bovine Serum Albumin
CMA	Chaperone Mediated Autophagy
CO ₂	Carbon Dioxide
DD	Death Domain
dH ₂ O	Distilled Water
DMEM	Dulbecco's Modified Eagle's Medium
DMSO	Dimethylsulphoxide
DNA	Deoxyribonucleic Acid
DPBS	Dulbecco's Phosphate Buffered Saline
ds	Double Stranded
ECL	Enhanced Chemiluminescence
EDTA	Ethylenediaminetetraacetic Acid
EGF	Epidermal Growth Factor
ER	Endoplasmic Reticulum
EtOH	Ethanol
FADD	Fas-Associated Death Domain
FasL	Fas Ligand
FBS	Foetal Bovine Serum
FITC	Fluorescein Isothiocyanate
GSK3	Glycogen synthase kinase 3
HSP	Heat Shock Protein
IL	Interleukin
IP3R	Inositol Triphosphate 3 Receptor

JNK	c-Jun N-terminal Kinase
LC3B	Light Chain Three Beta
MCF	Michigan Cancer Foundation
MeOH	Methanol
MMP	Mitochondrial Membrane Potential
MnSOD	Manganese Superoxide Dismutase
MTT	(3-(4,5-Dimethylthiazol-2-yl)-2,5-diphenyltetrazolium bromide)
n	Number of Experiments
NAD ⁺	Nicotinamide Adenine Dinucleotide
O ₂	Oxygen
PAK2	P21 (CDKN1A)-Activated Kinase 2
PARP	poly(ADP-ribose) polymerase
PBS	Phosphate Buffered Saline
pl	Propidium Iodide
PI3	Phosphatidyl Inositide 3
PMSF	Phenylmethylsulphonyl Fluoride
PVDF	Polyvinilidene Fluoride
RIP	Receptor Interacting Protein
RIPA	Radioimmunoprecipitation
RNA	Ribonucleic Acid
RT	Room Temperature
SDPBS	Staining Dulbecco's Phosphate Buffered Saline
SDS-PAGE	Sodium-dodecyl-sulphate-polyacrylamide gel electrophoresis
SEM	Standard Error of the Mean
ss	Single Stranded

TBS-T	Tris Buffered Saline-Tween 20
Temed	N,N,N,N' - Tetramethylethyldiamin
TNF	Tumour Necrosis Factor
Tris	Trizma® Base
UV	Ultraviolet

List of Tables

Table 3.1. Seeding densities

Table 3.2. Primary antibodies used for immunocytochemistry

Table 3.3. Secondary antibodies used for immunocytochemistry

Table 3.4. Primary antibodies used for protein detection

List of Figure Titles

Figure 1.1. Schematic representation of steps in the intrinsic and extrinsic pathways of apoptosis, leading to substrate cleavage and cell death. See text for details.

Figure 1.2. Schematic representation of the steps in necrosis leading to cell death. The process starts with receptor damage or signalling, after which excessive Ca^{2+} flux into the cell takes place. This leads to mitochondrial uncoupling, causing an increase in oxygen consumption, ATP depletion, and ROS generation. Perinuclear clustering of mitochondria take place, followed by calpain and cathepsin activation. The plasma membrane ruptures, leading to cell death.

Figure 1.3. The autophagic pathway. In the presence of adequate nutrients, growth factors are able to activate the class I PI3K proteins, which in turn signal via the AKT pathway to activate mTOR. This leads to an inhibition of ATG1 - the key signal in autophagy induction. If there are inadequate nutrients or in the presence of mTOR inhibitors, e.g. Rapamycin, mTOR is not activated and ATG1 is able to recruit ATG11, ATG13 and ATG17, to form a complex which signals induction of autophagy. Formation of the autophagosome is dependent on the formation of two complexes - ATG6 (Beclin-1), which interacts with the class III PI3K protein complexes with ATG14, and the second complex, which involves ATG12, ATG16, ATG5 and ATG7.

This complex is critical for the recruitment of ATG8 (LC3). Upon induction of autophagy, cytosolic LC3-1 (ATG8) is cleaved, and lipidated to form LC3-II. LC3 is a marker for the autophagosome membrane.

Figure 1.4. Schematic representation of chronological events in apoptosis, necrosis and autophagy, ending in cell death.

Figure 2.1. The structure of curcumin, its natural analogs and its most important metabolites in rodents and humans. Curcumin, when administered orally, undergoes glucuronidation and sulfation; when administered intravenously (i.v.) or intraperitoneally (i.p) it undergoes reduction that leads to the formation of tetrahydrocurcumin, hexahydrocurcumin and octahydrocurcumin (also known as hexahydrocurcuminol) (Aggarwal & Sung, 2008).

Figure 4.1.1 Viability in % showing control and treatment with curcumin of MCF-12A cells for a time period of 48 hrs using 10, 50, 100 and 200 μ M concentrations, n = 9.

Figure 4.1.2 Viability in % showing control and treatment with curcumin of MCF-7 cells for a time period of 48 hrs using 10, 50, 100 and 200 μ M concentrations. *p<0.05 vs Control, #p<0.05 vs 200 μ M, n=9.

Figure 4.2.1.1 MCF-12A cells labeled with LC3/FITC displayed in green, Beclin/TexRed displayed in red, and the nuclear indicator Hoechst, displayed in blue. The figure shows MCF-12A cells untreated, n = 3.

Figure 4.2.1.2 MCF-12A cells labeled with LC3/FITC displayed in green, Beclin/TexRed displayed in red, and the nuclear indicator Hoechst, displayed in blue. The figure shows MCF-12A cells treated with 200 μ M curcumin, n = 3.

Figure 4.2.1.3 MCF-12A cells labeled with caspase-3/TexRed displayed in red, and the nuclear indicator Hoechst, displayed in blue. The figure shows MCF-12A cells untreated (A-C) and treated (D-F), n = 3.

Figure 4.2.1.4 MCF-12A cells labeled with PARP/TexRed displayed in red and the nuclear indicator Hoechst, displayed in blue. The figure shows MCF-12A cells untreated (A-C) and treated (D-F), n = 3.

Figure 4.2.1.5 MCF-7 cells labeled with LC3/FITC displayed in green, Beclin/TexRed displayed in red, and the nuclear indicator Hoechst, displayed in blue. The figure shows MCF-7 cells untreated, n = 3.

Figure 4.2.1.6 MCF-7 cells labeled with LC3/FITC displayed in green, Beclin/TexRed displayed in red, and the nuclear indicator Hoechst, displayed in blue. The figure shows MCF-7 cells treated, n = 3.

Figure 4.2.1.7 MCF-12A cells labeled caspase-3/TexRed displayed in red and the nuclear indicator Hoechst, displayed in blue. The figure shows MCF-12A cells untreated (A-C) and treated (D-F), n = 3.

Figure 4.2.1.8 MCF-7 cells labeled with PARP/TexRed displayed in red and the nuclear indicator Hoechst, displayed in blue. The figure shows MCF-7 cells untreated (A-C) and treated (D-F), n = 3.

Figure 4.2.2.1 MCF-12A cells (left panel) and MCF-7 cells (right panel) incubated with Hoechst, displayed in blue, and Propidium iodide, displayed in red. Shown are untreated cells (A and B), vehicle controls (C and D) and treated cells (E and F), n = 3.

Figure 4.3.1 Schematic representation of Beclin-1 expression, in % of control in MCF-12A and MCF-7 cells, after no treatment, vehicle treatment, or treatment with 200 μ M curcumin, all for 48 hrs, n = 3.

Figure 4.3.2 Schematic representation of total caspase-3 expression, in % of control in MCF-12A and MCF-7 cells, after no treatment, vehicle treatment, or treatment with 200 μ M curcumin, all for 48 hrs, n = 3.

Figure 4.3.3 Schematic representation of cleaved caspase-3 expression, in % of control in MCF-12A and MCF-7 cells, after no treatment, vehicle treatment, or treatment with 200 μ M curcumin, all for 48 hrs, n = 3.

Figure 4.3.4 Schematic representation of Total PARP expression, in % of control in MCF-12A and MCF-7 cells, after no treatment, vehicle treatment, or treatment with 200 μ M curcumin, all for 48 hrs, n = 3.

Figure 4.3.5 Schematic representation of cleaved PARP expression, in % of control in MCF-12A and MCF-7 cells, after no treatment, vehicle treatment, or treatment with 200 μ M curcumin, all for 48 hrs, n = 3.

Figure 4.4.1.1 Acridine orange mean fluorescence intensity presented as a % of the control in MCF-12A cells, after no treatment, vehicle treatment, or treatment with 200 μ M curcumin, all for 48 hrs. *p<0.05 vs Control, #p<0.05 vs vehicle, n = 3.

Figure 4.4.1.2 Acridine orange mean fluorescence intensity presented as a % of the control in MCF-7 cells, after no treatment, vehicle treatment, or treatment with 200 μ M curcumin, all for 48 hrs. *p<0.05 vs Control, #p<0.05 vs vehicle, n = 3.

Figure 4.4.2.1 Hoechst mean fluorescence intensity presented as a % of the control in MCF-12A cells, after no treatment, vehicle treatment, or treatment with 200 μ M curcumin, all for 48 hrs.

Figure 4.4.2.2 Hoechst mean fluorescence intensity presented as a % of the control in MCF-12A cells, after no treatment, vehicle treatment, or treatment with 200 μ M curcumin, all for 48 hrs. *p<0.05 vs Control, #p<0.05 vs 200 μ M.

Table of Contents

	Pages
Chapter 1: Motivation for study	1
Chapter 2: Literature review	
2.1 Introduction	3
2.2 Modes of cell death	6
2.2.1 Introduction	6
2.2.2 Apoptosis	7
2.2.2 (a) <i>Role of caspases in apoptosis</i>	9
2.2.2 (b) <i>Role of PARP in apoptosis</i>	10
2.2.2 (c) <i>Regulatory proteins involved in apoptosis</i>	11
2.2.2 (d) <i>Markers of apoptosis</i>	15
2.2.3 Necrosis	15
2.2.3 (a) <i>Marker of necrosis</i>	20
2.2.4 Autophagy	20
2.2.4 (a) <i>Markers of autophagy</i>	21
2.3 The initiation of cell death in cancer	25
2.3.1 Apoptosis and cancer	25
2.3.2 Necrosis and cancer	26
2.3.3 Autophagy and cancer	26
2.4 Curcumin as a treatment modality in cancer	28
2.4.1 Apoptosis and curcumin	29
2.4.2 Autophagy and curcumin	30
2.4.3 Necrosis and curcumin	31
Chapter 3: Materials and Methods	
3.1 Cell Culture	32
3.1.1 <i>Cell lines</i>	32
3.1.2 <i>Cell culture procedure</i>	32
3.1.3 <i>Curcumin treatment</i>	33
3.2 MTT (3-(4,5-Dimethylthiazol-2-yl)-2,5-diphenyltetrazolium bromide) Assay	33
3.3 Immunocytochemistry	34
3.3.1 <i>Sample preparation</i>	34

3.3.2 <i>Propidium Iodide (PI)</i>	35
3.3.3 <i>Hoechst</i>	35
3.3.4 <i>Anti Beclin-1, PARP, LC3B, Caspase-3</i>	36
3.3.5 <i>Immunocytochemistry procedures</i>	37
3.4 Fluorescence microscopy	37
3.4.1 <i>PI and Hoechst</i>	37
3.4.2 <i>Anti Beclin-1, PARP, LC3B, Caspase-3</i>	38
3.5 Fluorescence activated cell sorting (FACS)	38
3.5.1 <i>Sample preparation</i>	38
3.5.2 <i>Hoechst</i>	39
3.5.3 <i>Acridine orange</i>	39
3.6 Methods of protein analysis	40
3.6.1 <i>Bradford protein quantification</i>	40
3.6.2 <i>Sodium-dodecyl-sulphate-polyacrylamide gel electrophoresis (SDS PAGE)</i>	40
3.6.3 <i>Film analysis</i>	43
3.7 Statistical methods	43
Chapter 4: Results	
4.1. MTT assay	45
4.2 Fluorescence microscopy	48
4.2.1. Antibody staining	48
4.2.2. Propidium iodide exclusion technique	54
4.3 Western Blots	56
4.4 Flow cytometry	62
4.4.1 Acridine orange staining	62
4.4.2 Hoechst staining	65
Chapter 5: Discussion and conclusion	68
References	75
Addenda 1-3	86

Chapter 1: Motivation for study

The importance of diet-derived agents in the maintenance of health and in the prevention and treatment of disease should not be underestimated. Based on published mortality data, one of the leading causes of death worldwide is malignant neoplasms. Over the past decade, a significant increase has been noted in public and scientific interest in the beneficial effects of chemicals derived from plants, known as phytochemicals, and their role in the maintenance of health and the prevention of disease. The term nutraceutical was coined in 1989 by Dr Stephen DeFelice, founder and chairman of the Foundation for Innovation in Medicine, Cranford, New Jersey, as a substance that is either a food, or is part of a food that provides medical or health benefits, including the prevention and treatment of disease.

By focusing on the development of targeted therapies for cancer, the possibility of high therapeutic efficacy, with minimal side effects, could be achieved. One of the major, yet still elusive ideals in contemporary anti-cancer drug development is to achieve therapeutic selectivity, or the preferential killing of cancer cells without noteworthy toxicity to normal cells. To achieve this, tumour cell-specific molecular pathways that are agreeable to drug development has to be identified, and the targeting of these pathways should lead to therapeutic response. An intangible goal in oncology thus far has been to advance the identification of such targets, preceding clinical testing (Polyak, 2007). Also, the limited progress achieved by cancer therapy in the last thirty years has shifted the focus to cancer chemoprevention through the use of orally administered chemicals with no or very low toxicity, aimed at healthy or predisposed populations (Parkin *et al.*, 2002; Jemal *et al.*, 2008).

Polyphenols are among the leading chemical substances that fulfil this definition. They are derived from many components of the human diet, including dark chocolate, peanuts, green and black tea, red wine, olive oil, and the spice turmeric. Curcumin, a natural occurring compound derived from turmeric, has long been suggested to have strong therapeutic or preventative potential against several major human diseases because of its anti-oxidative, anti-inflammatory and anti-cancerous effects.

In the past years it has become clear that, in addition to apoptosis and necrosis, autophagy also serves as a major role player in therapy-induced cell death. Given the wide variety of defects that can suppress cell death in most cancers, understanding the regulation and significance of the different forms of cell death, is of utmost importance.

Therefore, using cultured MCF-12 (normal breast epithelial cells) and MCF-7 cells (breast carcinoma cells) as a model, the aims of this study were:

- ▶ To determine the effect of curcumin on cell viability in MCF-12 and MCF-7 cells
- ▶ To establish the concentration of curcumin which will effectively kill cancer cells without harming normal cells.
- ▶ To determine the effect of curcumin on the cell cycle of MCF-12 and MCF-7 cells
- ▶ To determine the effects of curcumin on apoptosis, necrosis and autophagy

Before a study of this nature can be attempted, a thorough knowledge and insight into the processes of apoptosis, necrosis and autophagy are required. The current

understanding and knowledge of these aspects will now be addressed in the literature review.

Chapter 2: Literature Review

2.1 Introduction

Malignant neoplasms have afflicted people for numerous centuries. The oldest documented case of cancer dates back to ancient Egypt, 1500 b.C., and consists of a papyrus document in which eight cases of tumours occurring in the breast were described. Before techniques existed to unravel the molecular and cellular mechanisms behind the cause of cancer, it was believed that the disease was caused by the gods, and the method of tumour excision described does not differ greatly from current day practice - a cauterizing instrument termed "The Fire Drill" was used to remove the tissue. Notably, it was also recorded that no remedy for the disease existed, and that palliative management was the only option. Many years later, the term *carcinoma* was composed from the Greek terms *carcinos* and *carcinoma* by the Greek physician Hippokrates - words used to describe a crab or crayfish, the legs of which he thought to resemble the veins stretching over the cut surface of a malignant tumour. The word *oncos*, first used to describe malignant tumours, and later all tumours, is the root for the currently used term "oncology" (Karpozilos & Pavlidis, 2004).

Hippokrates and other early Greek physicians also believed that cancer was caused by an excess of black bile in any specific area of the body - black bile being the fourth of the fluids they thought the human body to consist of, the other three being blood, phlegm and yellow bile. Thereafter, the dogma of black bile being the source of cancer triumphed for more than 2000 years. Only as recently as the 18th century, as extensive use of the microscope became imminent, the process of metastasis was

observed and described between 1871 and 1874 by the British surgeon, Campbell De Morgan (Grange *et al.*, 2002).

Besides being largely ineffective and leading to many deaths due to sepsis, the use of surgery to remove tumours was still the most used form of treatment at this time. At the end of the 19th century, the foremost effective form of non-surgical treatment for cancer was discovered by Marie and Pierre Curie. This discovery had considerable repercussions in the sense that it led to patients having to be admitted to a hospital in order to receive treatment, which in turn led to the documentation of patient data and statistics in the form of hospital files. This contributed immensely to the scientific research effort to understand the processes of the disease and progress in the development of potential therapies. Advances made in research in 1975, concerning the proto-oncogene, was a profound step towards gaining insight into the molecular and cellular mechanisms implicated in the causation of human cancer (Jemal *et al.*, 2008).

However, over 3500 years after the first documented cases of cancer, the prevention, diagnosis and cure of human cancers still does not seem to be imminent. Doctrines have been clarified over the decades and have been applied to make headway, but with marginal success rates. In 2003 it was established that approximately one third of women with breast cancer eventually die from dissemination of the disease through metastasis. In the United States, cancer was responsible for approximately 25% of all deaths in 2005, with a total of 1 437 180 new cases of cancer and 565 650 mortalities from cancer projected to occur in 2008 (Jemal *et al.*, 2008).

Currently, breast cancer is the principal cause of cancer-related death in women globally (Kamangar *et al.*, 2006). Regardless of noteworthy progress being made in the diagnosing and treating of breast cancer, several major unresolved clinical and scientific challenges remain. Problems include: identifying suitable candidates for education regarding prevention, finding more specific and sensitive means of identification of the disease, pinpointing the cause of, and unravelling the mechanisms behind tumour progression and recurrence, selecting the right type of treatment per individual, and essentially, how to overcome therapeutic resistance. However, posing the largest problem is the fact that breast cancer is highly heterogenous at the molecular and clinical level (Perou *et al.*, 2000; Sorlie *et al.*, 2001). Although the precise aetiology of breast cancer still remains unspecified, family history is one of the strongest determinants of risk, which implies that the cause could also be hereditary (Polyak, 2007).

Recently, there has been noteworthy progress in the development of targeted therapy drugs that act exclusively on measurable molecular abnormalities in certain tumours, and minimizes injury to normal cells. The compound curcumin from *Curcuma longa* is believed to be such a substance. Curcumin, or diferuloylmethane, is a natural phytochemical and is presently under a great deal of inspection from cancer investigators because of its chemopreventative properties against human malignancies. Epidemiological data show that the incidence of cancers of the colon, breast, prostate and lungs are higher in Western countries than in countries such as India, where curcumin is exceedingly consumed (Aggarwal *et al.*, 2003; Parkin *et al.*, 2002). Furthermore, studies done on rodent models showed the preventative properties of curcumin against colon, lung, breast, liver, stomach, esophagus and

skin cancers. In a clinical trial done in persons with precancerous lesions, the oral administration of curcumin over a 3 month period led to histological improvement of lesions in seven of the 25 subjects (Cheng *et al.*, 2001). However, no literature exists regarding the effect of curcumin on the induction of different forms of cell death (apoptosis, autophagy and necrosis) in a model of breast cancer.

2.2 Modes of Cell Death

2.2.1 Introduction

Cell death constitutes one of the key events in medical research. Cellular homeostasis is maintained by a balance between cell proliferation and cell death. Our understanding of the mechanisms of cell death has vastly increased in the last decades with advances in molecular- and cell biology. Three main types of cellular catabolism can be defined according to morphological criteria, namely apoptosis (Type I, which is a form of programmed cell death), cell death associated with autophagy (Type II) and necrosis or oncosis (Type III).

Cells undergoing apoptosis show typical, well-defined morphological changes, including plasma membrane blebbing, chromatin condensation with margination of chromatin to the nuclear membrane, karyorhexis (nuclear fragmentation), and formation of apoptotic bodies (Kerr *et al.*, 1972). Apoptosis has been characterized by several biochemical criteria, including exposure of phosphatidylserine (PS) on the outer leaflet of the plasma membrane (Fadok *et al.*, 1992; Denecker *et al.*, 2001), changes in mitochondrial membrane permeability (Kroemer & Reed, 2000), the release of mitochondrial proteins from the intermembrane space (Van Loo *et al.*, 2002), and internucleosomal DNA cleavage (Enari *et al.*, 1998). Identification of

these morphological and biochemical markers of apoptosis makes it possible to distinguish it from other forms of cell death.

Cells undergoing death associated with autophagy are characterized by the presence of double membrane autophagic vacuoles. Autophagy is foremost a survival mechanism that is activated in cells subjected to nutrient or growth factor deprivation. When cell stress continues, cell death may continue by autophagy alone, or else it often becomes associated with features of apoptotic and necrotic cell death (Maiuri *et al.*, 2007). Specific biochemical markers have been developed to determine cell death associated with autophagy, such as the lipidation of LC3, as detected by band shift in western blots (Tanida *et al.*, 2004; Mizushima & Yoshimori, 2007), or delocalization of GFP-LC3 to the autophagosomes (Krysko *et al.*, 2008).

In contrast, necrosis is characterized by irreversible changes in the nucleus (karyolysis and pyknosis), and in the cytoplasm (condensation and intense eosinophilia, loss of structure and fragmentation). It culminates in rupture of the plasma membrane and organelle breakdown (Majno & Joris, 1995). Necrosis has long been described as a consequence of extreme stress on the cell, and therefore the cell death process has been described as accidental and uncontrolled. However, many different cellular stimuli (TNF- α , ATP depletion, ischemia) have been shown to induce a necrotic process that follows defined steps and signalling events reminiscent of a true death program (Vanden Berghe *et al.*, 2007).

2.2.2 Apoptosis

The ground breaking publication by Kerr *et al* in 1972, regarding a then obscure mode of programmed cell death they termed apoptosis, paved the way for one of the most rigorously studied topics in contemporary biology. They concluded that apoptosis is not only restricted to embryos as a mechanism for successful organogenesis and the development of multicellular tissues, as was previously believed, but that it also occurs in adult cells, and, moreover, that unsuccessful apoptosis contributes to a assortment of diseases, including cancer (Lockshin & Zakeri, 2001). The introduction of differentiated cell types as a result of evolution may have created a requirement for managing death as well as division in order to keep neighbouring cells co-dependent and insure the suitable stability of each cell lineage (Danial & Korsemeier, 2004).

Apoptosis is defined as a discrete sequence of morphological changes including cell shrinkage, membrane blebbing, cleavage of chromosomal DNA into internucleosomal fragments and chromatin condensing into heterochromatin in one or more bodies in the nucleus (Furth, 1999; Edinger & Thompson, 2004). Condensed chromatin typically settles alongside the nuclear membrane in a process called chromatin margination. As opposed to necrosis, cell membranes remain intact – apoptotic cells do not liberate their contents or influence the behaviour of adjacent cells, as is found during necrosis. Immune activation is avoided by packaged cell fragments being phagocytosed by surrounding cells (Boulares, 1999; Edinger & Thompson, 2003).

The molecular events of apoptosis can be separated into three processes or stages. Firstly, there is the initiation by an apoptosis-inducing agent. Secondly, a signal transduction cascade causes activation of the fundamental 'assassin' family of proteins, the caspases. Thirdly, proteolytic cleavage of cellular compartments occurs. Numerous death and survival genes managed by extracellular factors are engaged in the process, and different apoptosis-inducing agents activate different apoptosis-inducing pathways. For the purpose of this study, we shall focus on the role of the caspases in apoptosis.

Apoptosis occurs through two discrete cellular pathways, namely the extrinsic and the intrinsic pathways, respectively. The extrinsic pathway is activated by the binding of death activator proteins to the cell surface. The intrinsic pathway is instigated by signals originating from inside the cell, such as injury caused by ionizing radiation, toxins, the withdrawal of survival factors, such as growth factors and hormones, or by aberrations in the cell cycle. Both pathways come together inside the cell, triggering the caspases. These enzymes cut up proteins inside the cell and digest the cell from within (Edinger & Thompson, 2003).

2.2.2 (a) Role of caspases in apoptosis

Caspases are characterized by a cysteine active site with an aspartate substrate specificity. They subsist as proenzymes which consist of a prodomain and a catalytic protease domain. Caspases are classified as initiator, which cleave other caspases, or executioner caspases, which cleave a range of cellular proteins. Initiator caspases are caspases-3, -6 and -7, while caspases-8, -9, -10 and -12 are the executioner caspases.

The caspase cascade is activated by either two of the known aforementioned pathways. The intrinsic pathway engages the Bcl-2 family of proteins and the release of cytochrome c, a small heme protein which is a member of the cytochrome c family of proteins, found loosely associated with the inside of the mitochondrial membrane. However, the actions leading to the release of cytochrome c from the mitochondria are still poorly comprehended.

Nonetheless, it is known that the release of this protein initiates an interaction with the Inositol Triphosphate 3 receptor (IP3R) on the endoplasmic reticulum (ER), triggering ER calcium liberation. This increase in calcium sets off a vast release of cytochrome c, in turn taking effect in the positive feedback loop to sustain ER calcium release via the IP3Rs. In this manner, ER calcium release can reach cytotoxic levels. This release of cytochrome c sequentially activates caspase 9, a cysteine protease. Caspase 9 then proceeds to activate caspase 3 and caspase 7, which are accountable for dismantling the cell from within (Herr & Debatin, 2001).

The extrinsic pathway does not involve mitochondria, but is provoked by death receptor-protein complexes that cleave procaspase-8. Cleavage and activation of caspase-8 leads to launching of the caspase cascade. Following initial induction, the intrinsic and extrinsic pathways amalgamate at the level of the effector caspases. The effector caspases cleave DNA repair enzymes (eg. poly-ADP-ribose polymerase: PARP), nuclear and cytoskeletal proteins, as well as intracellular signalling molecules. The receptor pathway is connected to the mitochondrial pathway through cross-talk that takes place between the two pathways; caspase-8 cleaves the proapoptotic cytosolic protein Bid, which then translocates to the mitochondria and

binds to bad, an additional proapoptotic protein, ensuing in the release of cytochrome c and the activation of Apaf-1 (Poulaki *et al.*, 2001; Kasibhatla & Tseng, 2003).

2.2.2 (b) Role of PARP in apoptosis

Poly (ADP-ribose) polymerase-1 or PARP-1 is a nuclear enzyme which is copiously expressed in the nucleus and prompts the release of potent mitochondrial cytotoxins that promote apoptosis. Approximately one molecule of PARP-1 is expressed per 1000 DNA base pairs. PARP-1 catalyzes the transformation of β -nicotinamide adenine dinucleotide (NAD⁺) into nicotinamide and poly (ADP-ribose). Under homeostatic conditions, PARP-1 partakes in genome repair, DNA replication, and the management of transcription (Germain, 1999). In response to stress that are lethal to the genome, PARP-1 activity increases substantially, a fundamental event for maintaining genomic integrity (Shall & de Murcia, 2000). However, massive PARP-1 activation can deplete the cell of NAD⁺ and ATP, ultimately leading to energy malfunction and cell death (Ha & Snyder, 2000). The discovery that cell death may be stifled by PARP-1 inhibitors, or by deletion of the *parp-1* gene, prompted an upsurge of interest in the process of poly (ADP-ribosyl)ation. That PARP-1 might directly trigger apoptosis is supported by the observations of poly(ADP-ribose) production early in apoptotic cell death, and the increase in cell survival after deletion of the *parp-1* gene (Boulares *et al.*, 1999). PARP-1 action also triggers release of the mitochondrial pro-apoptotic protein called apoptosis-inducing factor (AIF) that promotes programmed cell death via a caspase independent pathway (Yu *et al.*, 2002.)

2.2.2 (c) Regulatory proteins involved in apoptosis

In apoptosis, protein-protein interactions are the underlying theme in both mitochondria and death receptor pathways. A sophisticated and tightly controlled network of protein-protein interactions exists to ensure the accuracy of the cell-death machinery.

The IAP (Inhibitor of apoptosis protein) family is another family of proteins that inhibits apoptosis through physically interacting with caspases and thereby directly inhibiting their function. The Bcl-2 family is a large key group of apoptosis regulators which, through the diverse interactions among themselves and with other proteins, control the release of apoptogenic factors needed for caspase activation (Adams & Cory, 1998; Chao & Korsmeyer, 1998). The Bcl-2 and IAP families are regulators of caspases at two different levels: the Bcl-2 family controls signalling events upstream of caspases, while the IAP family directly binds and inhibits caspases. The human IAP family contains eight distinct cellular members that were just discovered in the past 5-6 years, including X-IAP (X-linked IAP), c-IAP1, c-IAP2, and survivin (Devereaux *et al.*, 1999). In humans, IAPs such as X-IAP, c-IAP1, and c-IAP2 selectively inhibit caspase-3, -7 and -9 through direct molecular interactions but not caspase-1, -6, -8, -10. In addition, IAPs can interact with Smac/DIABLO, which is released from the mitochondria together with cytochrome c upon death stimuli. The binding of Smac/DIABLO removes IAPs from their association with caspases and thus relieves their caspase-inhibiting function (Devereaux *et al.*, 1997; Roy *et al.*, 1997).

Members of the Bcl-2 family include both anti-apoptotic proteins, exemplified by Bcl-2, Bcl-X_L, Mcl-1, Bcl-w and A-1, and pro-apoptotic proteins exemplified by Bax, Bak,

Bik, Bad and Bid. In terms of sequence, Bcl-2 family proteins share at least one of four homologous regions termed Bcl homology (BH1 to BH4). Based on sequence homology, a subclass of pro-apoptotic proteins termed “BH3-only” can be classified that share sequence homology only in the BH3 domain. While all of the pro-apoptotic members use the BH3 domain to interact with anti-apoptotic proteins, BH3-only proteins, including Bad and Bid, appear to act mainly as antagonists of anti-apoptotic members such as Bcl-2 and Bcl-X_L. In contrast to the opposing biological functions and wide differences in amino-acid sequences, experimentally determined crystal structures of Bcl-2 (Petros *et al.*, 2001) and Bcl-X_L (Muchmore *et al.*, 1996; Aritomi *et al.*, 1997), vs Bax (Suzuki *et al.*, 2000) and Bid (McDonnell *et al.*, 1999; Chou *et al.*, 1999) are surprisingly similar.

The mechanism by which Bcl-2 family proteins regulate apoptosis has been a subject of intensive research. Currently it remains controversial and several models have been proposed. An attractive mode of action is the heterotrimerization between anti-apoptotic and pro-apoptotic Bcl-2 family members (Reed, 1996; Yang *et al.*, 1995; Oltvai *et al.*, 1993). Some information about the structural basis of these interactions is provided by the three-dimensional structure of Bcl-X_L in complex with a peptide derived from the BH3 domain of Bak (Sattler *et al.*, 1997). The structure reveals a hydrophobic surface pocket on Bcl-X_L formed by the BH1-3 domains bound by the Bak BH3 domain peptide in helical conformation. Since the BH3 domain is buried in the structure of pro-apoptotic proteins Bid (McDonnell *et al.*, 1999; Chou *et al.*, 1999) and Bax (Suzuki *et al.*, 2000), this raises the speculation that conformational changes are necessary for the exposure of the BH3 domain of a pro-apoptotic protein and its inhibition of the functional pocket on the anti-apoptotic partner. In the cell

environment, pro-apoptotic Bcl-2 family members are suggested to undergo such conformational changes (Desagher *et al.*, 1999) triggered by dephosphorylation (Zha *et al.*, 1996) or proteolytic cleavage by caspases (such as the cleavage of Bid to generate tBid) (Slee *et al.*, 2000; Li *et al.*, 1998; Luo *et al.*, 1998).

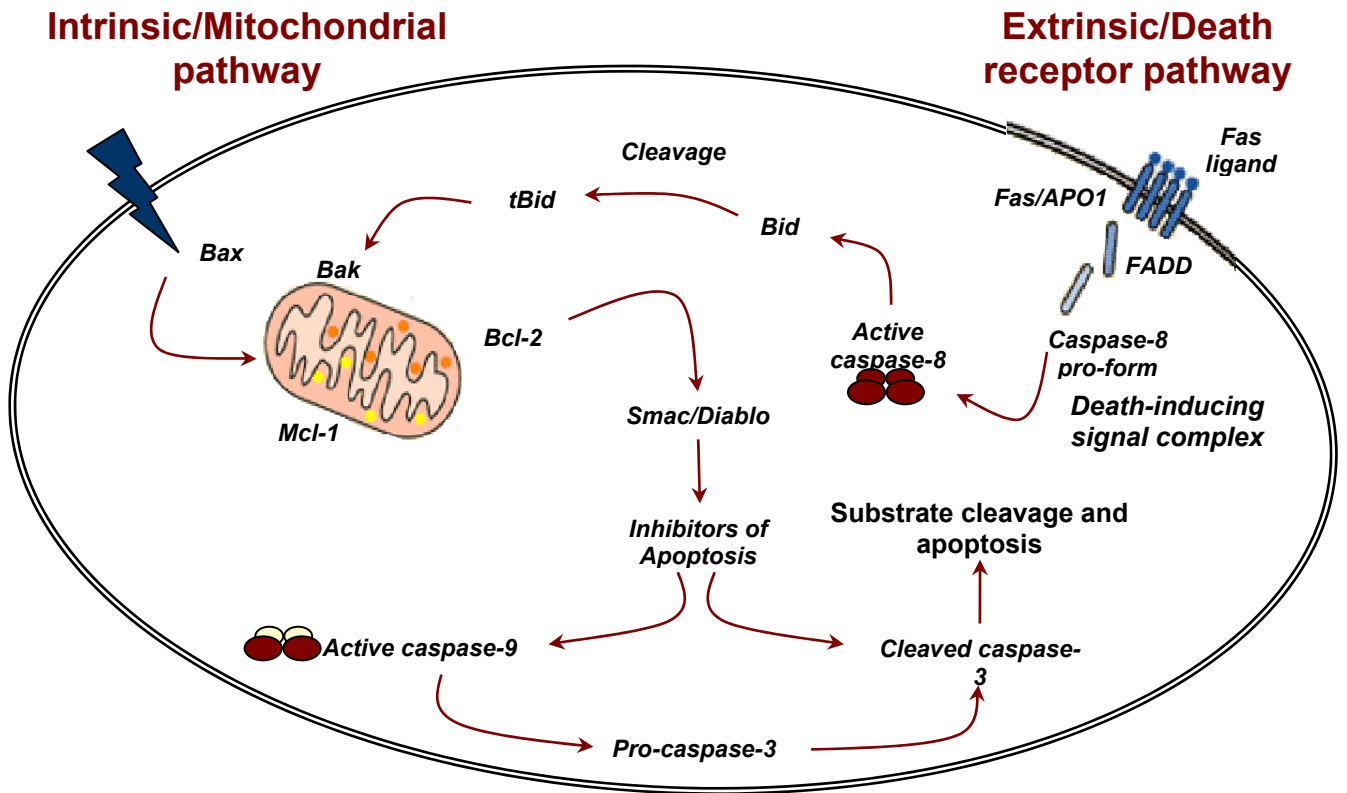


Figure 1.1 Schematic representation of steps in the intrinsic and extrinsic pathways of apoptosis, leading to substrate cleavage and cell death (original diagram). See text for details.

2.2.2 (d) Markers of apoptosis

Acridine Orange (AO) is a metachromatic dye which differentially stains double-stranded (ds) and single stranded (ss) nucleic acids. When AO intercalates into dsDNA it emits green fluorescence upon excitation at 480-490 nm. On the contrary, it emits red fluorescence when it interacts with ssDNA or RNA. Chromatin condensation is an early event of apoptosis and the condensed chromatin is more sensitive to DNA denaturation than normal chromatin. Therefore, if RNA is removed by pre-incubation with RNase A and DNA is denatured *in situ* by exposure to HCl shortly before AO staining, apoptotic cells (which have a larger fraction of DNA in the denatured form) display an intense red fluorescence and a reduced green emission when compared to non-apoptotic interphase cells (Hotz *et al.*, 1992; Gorman *et al.*, 1994).

Apoptotic cells, due to a change in membrane permeability, also show an increased up-take of the vital dye Hoechst 3334, compared to live cells. Propidium iodide (PI) is added to discriminate late apoptotic or necrotic cells which have lost membrane integrity from early apoptotic cells which still have intact membranes by dye exclusion (Ormerod *et al.*, 1992; Schmid *et al.*, 1994)

2.2.3 Necrosis

Necrosis is morphologically categorized by vacuolization of the cytoplasm, breakdown of the plasma membrane and the introduction of inflammation around the cell. These manifestations are ascribed to the release of pro-inflammatory molecules and the contents of the cell. Necrotic cells recurrently display modifications in nuclear morphology, but nothing resembling the organized chromatin condensation and

fragmentation of DNA as is seen in apoptotic cell death. Necrosis is also characterized by irrevocable changes in the nucleus, including karyolysis, pyknosis and karyorrhexis. Condensation and severe eosinophilia, loss of structure and disintegration of the cytoplasm also take place (Majno & Joris, 1995).

Recent studies imply that necrosis, which has always been thought of as an accidental form of cell death, might be programmed. When caspases were initially recognized as mediators of apoptosis, it was proposed that several of their substrates were crucial proteins whose obliteration made cell death inevitable. However, caspase-independent cell death is observed in many systems, which shows that cells could still die in the absence of their executioner. After an apoptotic stimulus, such as Bax expression, tumour necrosis factor (TNF) or Fas ligand treatment, cells die even in the presence of non-specific caspase inhibitors such as zVAD-fmk or anti-apoptotic molecules like Bcl-XL that prevent caspase activation (Lockshin & Zakeri, 2004; Jaattela & Tschopp, 2003). Under these circumstances, cells that would normally die by apoptosis, show all the hallmarks of necrosis.

In some cases, caspase-independent necrotic cell death can be averted by antioxidant treatment, or by eradicating the activity of the protein kinase receptor interacting protein (RIP). These results led to the idea that necrosis could be 'programmed' - cellular signalling events initiated necrotic destruction could be blocked by inhibiting discrete cellular processes. A criticism of this concept of necrosis as a programmed event has been that this form of cell death is only observed when apoptosis is inhibited - either genetically or chemically. In fact, recent evidence suggests that the initiation of apoptosis might actively suppress necrosis because activated caspases cleave and inactivate proteins required for programmed

necrosis (RIP and PARP) (Holler *et al.*, 2000; Ha & Snyder, 1999; Vercaemmen *et al.*, Zong *et al.*, 2004).

Moreover, the poor understanding of the definite mechanism(s) for necrotic cell death has contributed to denounce the notion of programmed necrosis as a tissue culture phenomenon.

Programmed necrosis could also be important in defending multicellular organisms from cells that have protracted DNA damage. It appears that an intact apoptotic pathway is not essential for the elimination of proliferating cells that acquire DNA damage, although this type of damage can initiate apoptosis (Zong *et al.*, 2004). In consequence, even cells that have a weakened apoptotic response can still be removed when confronted with attaining fixed mutations.

The DNA repair protein PARP was found to initiate programmed necrosis in response to DNA damage, but unexpectedly this form of cell death only occurred in actively proliferating cells. This discernment was accredited to the fact that PARP activation leads to the speedy exhaustion of nuclear and cytoplasmic NAD and consequently the inhibition of glycolysis. As a result, cells relying on glycolysis for ATP production rapidly become depleted of ATP after PARP activation and then die by necrosis. Proliferating, and in particular, transformed cells, are reliant on glucose metabolism for ATP production as they make use of amino acids and lipids for protein- and membrane synthesis, respectively. Conversely, quiescent cells can maintain ATP levels by means of oxidative phosphorylation by catabolising amino acids and lipids. In this case, PARP activation can endorse DNA repair and amend the damage without lethally depleting cellular ATP. Thus, PARP activation might administer a metabolic test on cells that have sustained DNA damage to determine

the degree of DNA damage and the possibility that mutations could be amplified by replication without repair. Therefore, acute and massive DNA damage induces hyperactivation of PARP leading to NAD⁺/ATP depletion, which eventually causes necrosis (Zong *et al.*, 2004).

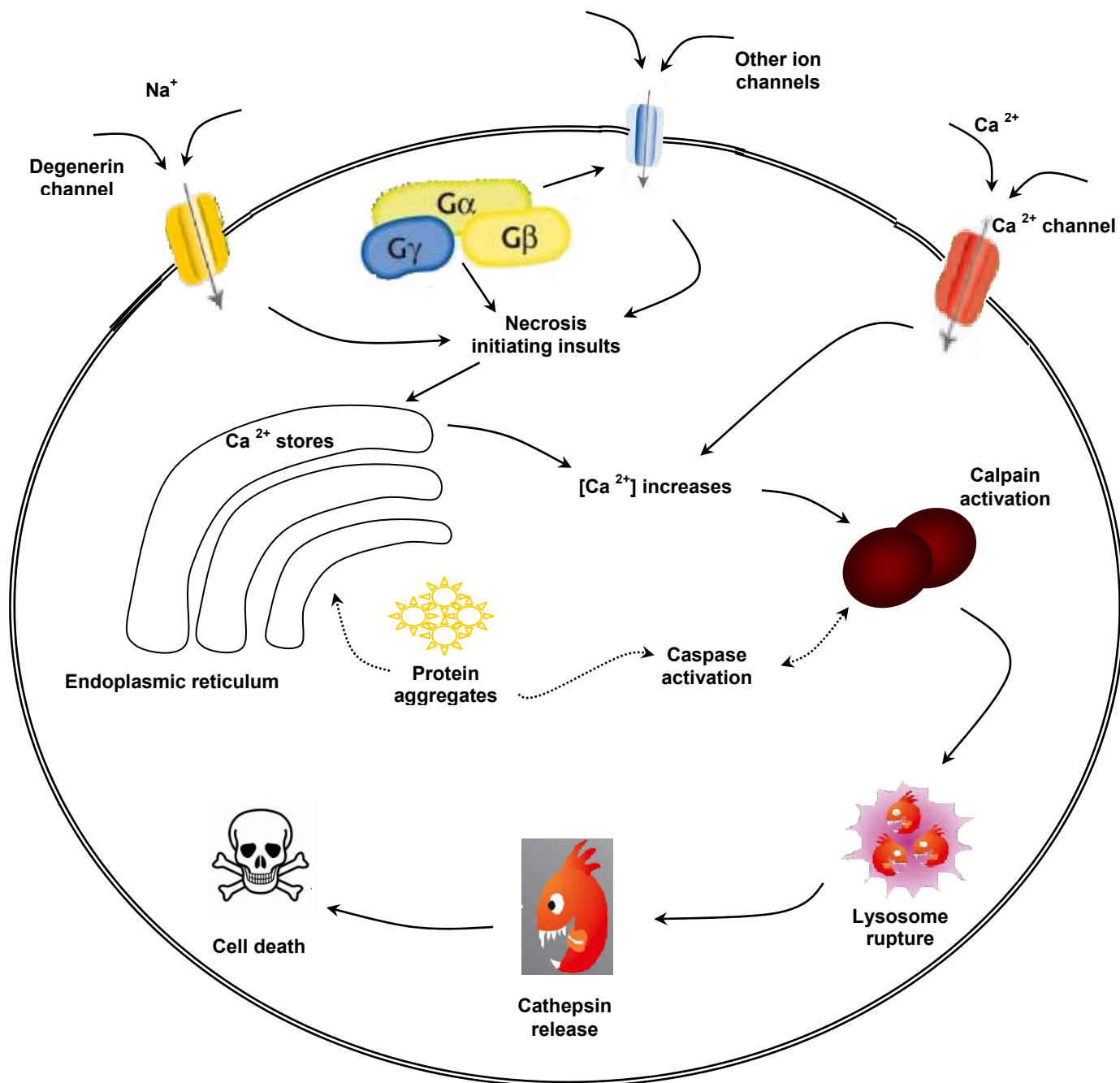


Figure 1.2 Schematic representation of the steps in necrosis leading to cell death (original diagram).

The process starts with receptor damage or signalling, after which excessive Ca^{2+} flux into the cell takes place. This leads to mitochondrial uncoupling, causing an increase in oxygen consumption, ATP depletion, and ROS generation. Perinuclear clustering of mitochondria take place, followed by calpain and cathepsin activation. The plasma membrane ruptures, leading to cell death.

2.2.3 (a) Marker of necrosis

A PI (Propidium Iodide) exclusion technique is used as an indication of changes in membrane integrity, and is based on the principle that PI can only enter the nucleus of a cell once the membrane integrity has been compromised (Vindelov *et al.*, 1983).

2.2.4 Autophagy

The process of autophagy was first described in the 1960's, whereafter Schweichel and Merker documented similar observations in embryonic and foetal tissues of rodents, in 1973. However, their findings were largely ignored and only once their classification was reassessed and expanded by Clarke in 1990, autophagy was recognized as a form of cell death (Gozuacik & Kimchi, 2004).

Autophagy, or 'self-eating' is defined as a catabolic process involving the degradation of a cell's own components through the lysosomal machinery. It is a tightly regulated process that plays a role in cell growth, homeostasis and development, and assisting to maintain a balance between the synthesis, break-down, and ensuing recycling of cellular products. It is a key mechanism through which a near-dying cell reorders nutrients from unnecessary processes to critical processes. A variety of autophagic processes exist, all sharing the same trait - the degradation of the intracellular components via the lysosome.

Three types of autophagy exist. Firstly, chaperone-mediated autophagy (CMA), which is a mechanism that allows the degradation of cytosolic proteins that contain a particular pentapeptide consensus motif. The cytosolic proteins are recognized by the binding of a heat shock protein 70 (hsc70) -containing chaperone/co-chaperone complex. The CMA substrate-chaperone complex then shifts to the lysosomes,

where it is recognized by the CMA receptor lysosome-associated membrane protein type-2A. The protein is unfolded and translocates across the lysosome membrane supported by the lysosomal hsc70 on the other side.

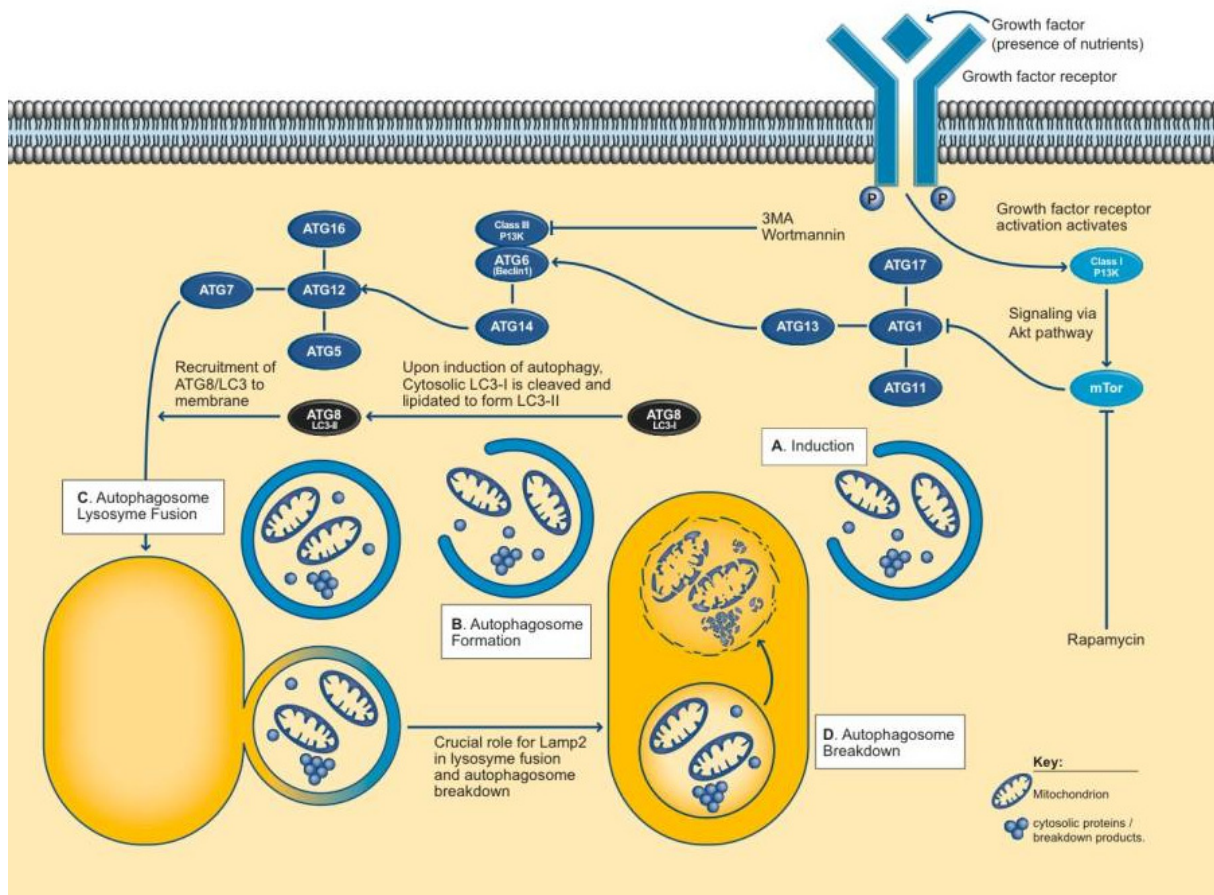
Secondly, microautophagy, which occurs when lysosomes directly swallow up cytoplasm by invagination, protrusion and/or septation of the lysosomal limiting membrane.

The third type, namely macroautophagy, is the autophagic process of interest in this study. Macroautophagy is the requisition of organelles and long-lived proteins in a double-membrane vesicle, called an autophagosome, inside the cell. Small membrane structures known as autophagosome precursors elongate to form autophagosomes. The formation of autophagosomes is initiated by class III PI3-kinase and autophagy-related gene Atg6, more commonly known as *Beclin-1*. In addition, two further structures are engaged, composed of the ubiquitin-like protein Atg8, more commonly known as light chain 3 (LC3), and the Atg4 protease on the one hand and the Atg12-Atg5-Atg-16 complex on the other (Schmid & Muenz, 2007). The outer membrane of the autophagosome fuses with a lysosome in the cytoplasm, forming an autolysosome or autophagolysosome where their contents are degraded via acidic lysosomal hydrolases (Gozuacik & Kimchi, 2004; Rubinsztein et al., 2005).

2.2.4 (a) Markers of autophagy

Beclin-1 initiates the formation of autophagosomes and is therefore critical to the process of autophagy. *Beclin-1* is generally ubiquitously expressed, but is mono-allelically deleted in the MCF-7 cell line. The presence of *Beclin-1* in MCF-7 cells is therefore considered to be indicative of autophagy (Liang et al., 1999).

LC3 is cleaved during autophagy to produce a cytosolic form, LC3-1. During autophagy, LC3-1 is converted to LC3-II through lipidation by an ubiquitin-like system involving Atg7 and Atg3 that allows for LC3 to become associated with autophagic vesicles. Thus, the presence of LC3 in autophagosomes as well as the conversion of LC3 to the lower migrating form LC3-II is considered to be indicative of autophagy.



(Reference: Abcam website: www.abcam.com)

Figure 1.3 The autophagic pathway. In the presence of adequate nutrients, growth factors are able to activate the class I PI3K proteins, which in turn signal via the AKT pathway to activate mTOR. This leads to an inhibition of ATG1 - the key signal in autophagy induction. If there are inadequate nutrients or in the presence of mTOR inhibitors, e.g. Rapamycin, mTOR is not activated and ATG1 is able to recruit ATG11, ATG13 and ATG17, to form a complex which signals induction of autophagy. Formation of the autophagosome is dependent on the formation of two complexes - ATG6 (Beclin-1), which interacts with the class III PI3K protein complexes with ATG14, and the second complex, which involves ATG12, ATG16, ATG5 and ATG7.

This complex is critical for the recruitment of ATG8 (LC3). Upon induction of autophagy, cytosolic LC3-1 (ATG8) is cleaved, and lipidated to form LC3-II. LC3 is a marker for the autophagosome membrane.

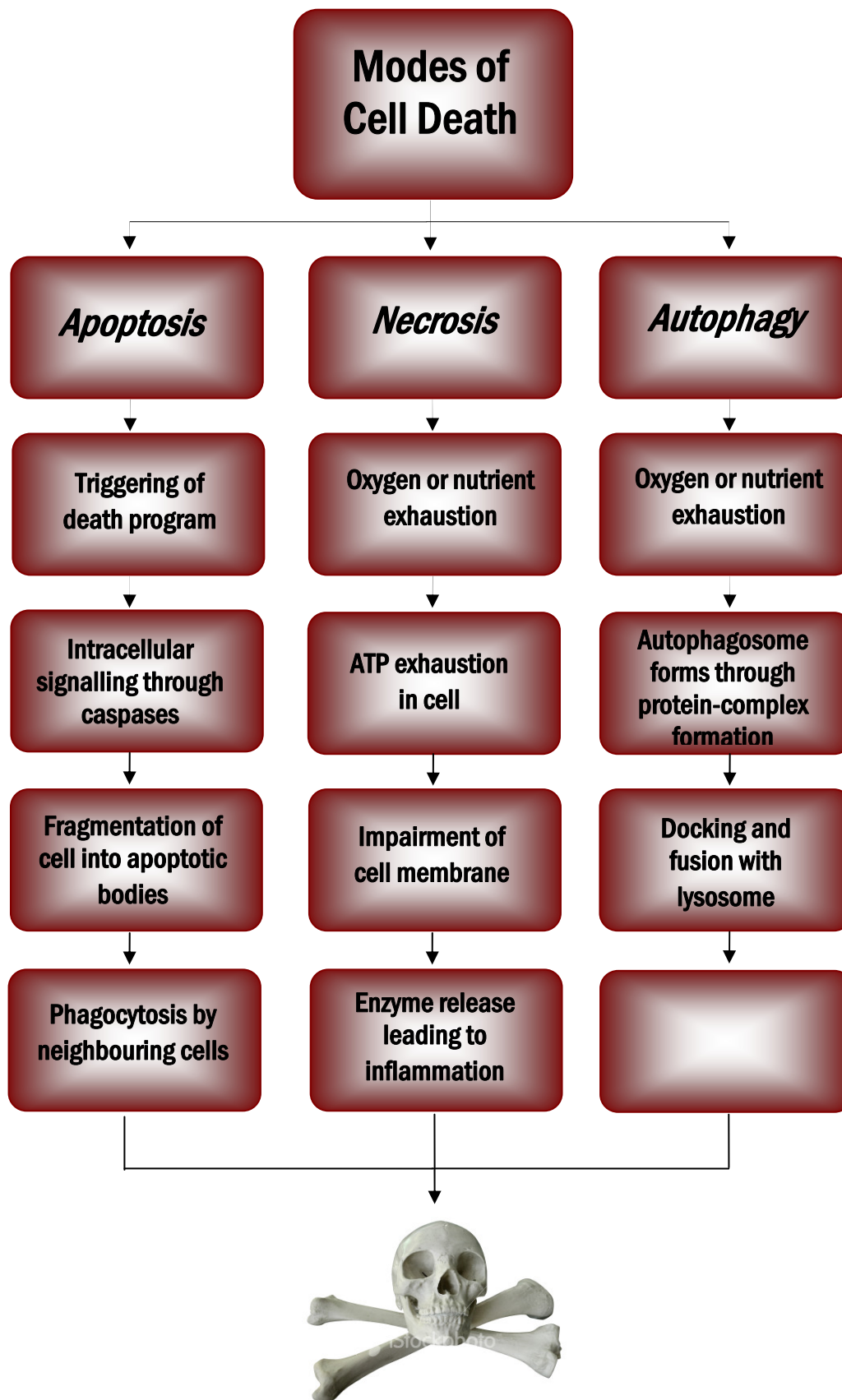


Figure 1.4 Schematic representation of chronological events in apoptosis, necrosis and autophagy, ending in cell death (original diagram).

2.3 The initiation of cell death in cancer

2.3.1 Apoptosis and cancer

In 1988, Vaux *et al.* verified that the *bcl-2* gene specifically impedes death of B cells in follicular lymphoma – therewith founding the relationship between apoptosis and cancer. Furthermore, in 1990, Korsmeyer and co-workers categorized *bcl-2* as a gene that inhibits suicide by producing a protein that hinders apoptosis. These findings established that tumours did not only develop from increased cell division, but also as a result of avoiding programmed cell death. Shortly thereafter, it also came to light that *bcl-2* hampers apoptosis by acting before cytochrome c is released from the mitochondria.

Evidence that this attained ability to resist apoptosis is a hallmark of possibly all forms of cancer, is increasing. Newly developed apoptosis-inducing drugs include Genasense™, which renders cancer cells more susceptible to apoptosis-inducing chemotherapies by barring the *bcl-2* protein, and Velcade™, which impedes activity of the cell's proteasome. Seeing that the proteasome acts as the exclusion agent for irregular, old or injured proteins, protein accumulates within the cell as a result of the inactivated proteasome. One of the accumulating proteins is BAX, which normally upholds apoptosis by obstructing the activity of *bcl-2*. As BAX concentrations amplify in reaction to Velcade, BAX inhibition of *bcl-2* also increases and the cell undergoes apoptosis in due course (Adams & Kauffman, 2004).

2.3.2 Necrosis and cancer

Many, if not all, human tumours harbour mutations that inactivate apoptotic pathways, granting tumour cells the opportunity to endure, despite of growing past homeostatic limits. Accordingly, the suggestion that tumour cells might be especially sensitive to programmed necrosis, could partly explain how certain targeted chemotherapeutics induce tumour cell death. For example, Okada *et al.* (2001) showed that BCR-ABL-positive leukaemia cells can undergo caspase-independent cell death in response to treatment with the Abl kinase inhibitor, Gleevec™ (Imatinib). This drug has been gratefully received as it is the first logically designed, effective cancer chemotherapeutic. Imatinib-induced necrotic cell death draws a parallel with the release of HtrA2/Omi, a serine protease, which is a known potential mediator of caspase independent necrotic cell death (Suzuki *et al.*, 2001). This type of cell death was blocked by treatment with serine protease inhibitors. The inflammatory constituent of necrotic death has the potential benefit of fuelling an immune response that could increase the effectiveness of Gleevec™ therapy. Whether Gleevec's™ efficacy is enhanced *in vivo* by an inflammatory reaction is not yet clear. Adjusting the balance between necrotic and apoptotic cell death, could possibly be a mechanism to enhance the eradication of tumour cells.

2.3.3 Autophagy and cancer

Autophagy was first linked to cancer by Levine and co-workers through their work on the identification and description of the *beclin 1* gene (Liang *et al.*, 1999). Poor vascularisation in solid tumours brings about nutrient, growth factor and oxygen deprivation, which in turn exerts severe metabolic stress on the tumour. Solid

tumours with defects in apoptosis have the ability to survive this, and autophagy localizes to the central and most metabolically deprived hypoxic tumour domain (Jin, 2006; Qu *et al.*, 2003; Tsukada & Ohsumi, 1993).

Negotiating autophagy in apoptosis-defective tumour cells considerably lessens the chance of survival in metabolic stress conditions *in vitro* and *in vivo*, establishing that autophagy is a survival pathway exploited to uphold viability during stages of nutrient limitation (Qu *et al.*, 2003). It has been shown that autophagy functions to sustain metabolism during times of growth factor deprivation of hematopoietic cells and during nutrient deprivation in normal mouse development (Balsara *et al.*, 2001; Bando *et al.*, 2000).

However, flaws in autophagy are associated with amplified tumourigenesis: human breast, ovarian and prostate tumours have allelic loss of the essential autophagy gene *beclin1* with high frequency and it was also observed that *beclin1* heterozygous mutant mice are tumour prone (Chen *et al.*, 1996; Cleton-Jansen *et al.*, 2001; Elo *et al.*, 1997). Moreover, *beclin1*^{+/-} immortal epithelial cells that exhibit heightened susceptibility to metabolic stress are also more tumorigenic than their *beclin1*^{+/+} equivalent, and this tumourigenicity is greatly intensified by an apoptosis defect (Qu *et al.*, 2003).

There is evidence for a role for autophagy in the eradication of damaged or faulty organelles, predominantly the mitochondria (Komatsu *et al.*, 2005; Feng *et al.*, 2005). Mitochondrial quality control may be crucial for preventing oxidative damage via the generation of reactive oxygen species. This could suggest that autophagy is needed not only as an alternate process of generating ATP during times of starvation, but that it also serves a function in maintaining homeostasis through protein and

organelle quality control. These functions may be especially vital in periods of metabolic stress, where ATP is limited and cellular damage accumulates rapidly. Autophagy might be particularly critical in tumours which are frequently subjected to stress (Li *et al.*, 1997). Tumours frequently lack the means for the complete elimination of damaged cells, which then ensures the safeguarding of damaged cells that could further contribute to tumour progression (Jin, 2005).

2.4 Curcumin as a treatment modality in cancer

One of the fundamental goals of cancer research should be to identify therapies that induce selective cancer cell death without harming normal cells. Understanding the processes that contribute to cell death and survival is critical in reducing morbidity and mortality from cancer. The extensive characterization of the regulatory factors involved in cell death will allow the development of targeted therapies and biomarkers.

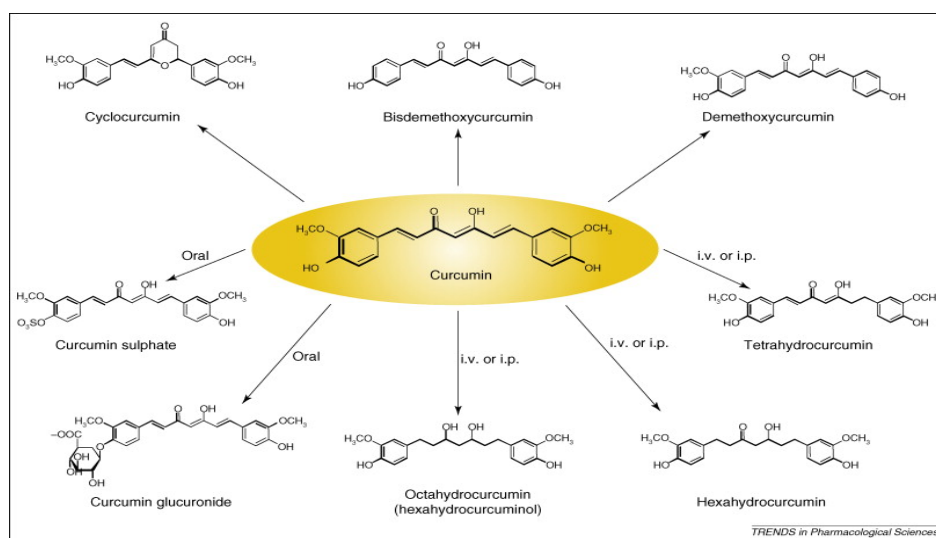


Figure 2.1. The structure of curcumin, its natural analogs and its most important metabolites in rodents and humans. Curcumin, when administered orally, undergoes glucuronidation and sulfation; when administered intravenously (i.v.) or intraperitoneally (i.p) it undergoes reduction that leads to the formation of tetrahydrocurcumin, hexahydrocurcumin and octahydrocurcumin (also known as hexahydrocurcuminol) (Aggarwal & Sung, 2008).

2.4.1 Apoptosis and Curcumin

Apoptotic cell death machinery in melanoma cells is modulated by curcumin through activation of caspases-3 and -8, but not caspase-9. Curcumin also stimulates the Fas receptor accumulation in a FasL-independent way, and expression of dominant negative Fas-Associated protein with Death Domain (FADD), the adaptor molecule, significantly inhibited curcumin-induced cell death (Bush *et al.*, 2001).

Curcumin also stimulates UV irradiation-induced and photosensitization-related apoptotic changes, including c-Jun N-terminal kinase (JNK) activation, loss of mitochondrial membrane potential (MMP), mitochondrial release of cytochrome c, caspase-3 activation, and cleavage/activation of PAK2 in human epidermoid carcinoma A431 cells (Chan *et al.*, 2003). The role of the NF- κ B signalling pathway in curcumin-mediated apoptosis has been clarified in studies in head and neck squamous cell carcinoma (Aggarwal *et al.*, 2004), mantle cell lymphoma (Shishodia *et al.*, 2005), lung cancer (Shishodia *et al.*, 2003), melanoma cells (Siwak *et al.*, 2005), cardiomyocytes (Yeh *et al.*, 2005; Yeh *et al.*, 2005), and liver cancer (Notarbartolo *et al.*, 2005). Parallel observations were also made in animal model systems - curcumin was found to have both pro- apoptotic and anti-angiogenic effects, implying its value as a capable chemotherapeutic agent (Belakavadi *et al.*, 2005). Mechanisms of curcumin-induced apoptotic effects were also seen in T-cell acute lymphoblastic leukaemia malignant cells in which curcumin repressed constitutively activated targets of the PI3-kinase (AKT, FOXO and GSK-3) pathway, causing reduced proliferation and induction of caspase-dependent apoptosis (Hussain *et al.*, 2006).

The majority of recent studies have indicated that curcumin is an effective therapeutic agent which suppresses anti-apoptotic factors, and activate calpain and caspase proteolytic cascades for apoptosis in human malignant glioblastoma cells (Karmakar *et al.*, 2006; Karmakar *et al.*, 2007).

In addition, p53 protein also plays an imperative role in mediating apoptosis through the activation of the death receptor and the mitochondrial apoptotic pathways (Shoba *et al.*, 1998). Also, it has been proven that the serine phosphorylation of p53 is up-regulated by curcumin in a concentration- and time-dependent manner (Song *et al.*, 2005; Tsvetkov *et al.*, 2005). Together, all these studies demonstrated that curcumin mediates its effects through varied growth regulatory mechanisms in tumour cells, therefore, curcumin shows justifiable promise as a multi-targeted drug in the management of human cancers.

2.4.2 Autophagy and curcumin

Two well known pathways which regulate autophagy in response to starvation are: the class I phosphatidylinositol 3-phosphate kinase/Akt/mammalian target of rapamycin (mTOR)/p70 ribosomal S6 kinase (p70S6K) signalling pathway and the Ras/Raf-1/mitogen-activated protein kinase 1/2 (MEK1/2)/extracellular signal-regulated kinase 1/2 (ERK 1/2) pathways (Codogno & Meijer, 2005; Meijer & Codogno, 2004). The Akt/mTOR pathway negatively regulates autophagy, whereas the ERK1/2 pathway positively regulates autophagy. Aoki and co-workers have demonstrated that curcumin inhibited the growth of human malignant glioma cells *in vitro* and *in vivo* by inducing autophagic cell death instead of apoptosis (Aoki *et al.*, 2007). They have demonstrated that curcumin induced autophagic cell death through

the inhibition of the Akt/mTOR/p70S6K pathway and through the simultaneous activation of the ERK 1/2 pathway.

2.4.3 Necrosis and curcumin

Although no direct evidence exists for the induction of necrosis by curcumin, it is known that within the same tumour necrosis, autophagy and apoptosis may co-exist, and the relative contribution of these three processes can dictate the trajectory of the tumour growth or regression as well as the host response.

Chapter 3: Materials and Methods

3.1 Cell Culture

3.1.1. Cell Lines

The Michigan Cancer Foundation-7 (MCF-7) cell line was a gift from Dr. Anne Louw, Department of Biochemistry, University of Stellenbosch, Stellenbosch, South Africa. MCF-7 is an invasive ductal breast carcinoma cell line, derived from a pleural effusion performed on a 69 year old Caucasian female in 1973 (Burdall, *et al.*, 2003).

The Michigan Cancer Foundation-12A (MCF-12A) cell line was a gift from Dr. Virna Leaner, Department of Medical Biochemistry, University of Cape Town Medical School, Observatory, South Africa. MCF-12A is a non-tumorigenic epithelial cell line, established from tissue taken at reduction mammoplasty from a 60 year old Caucasian female.

3.1.2 Cell culture procedure

For standard maintenance of cultures, cells were seeded into tissue culture flasks at a density of 4000 per cm² in the specified medium and incubated at 37°C, 95% humidity and 5% CO₂. Cultures were passaged at 70% confluency by washing with sterile DPBS, trypsinizing with 0.25% Trypsin-EDTA for 3 minutes at 37°C and centrifuging at 1300 revolutions per minute in a digicen20-R centrifuge for 3 minutes. The supernatant was carefully decanted and the pellet thoroughly resuspended in warm medium to achieve a single cell suspension. Cells were then reseeded, and never passaged more than ten times. For experimental purposes, cells were seeded as follows:

Table 3.1. Seeding densities

Type of Analysis	Culture Dish	MCF-7	MCF-12A
MTT Assay	12-Well Plates	80 000 Per Well	40 000 Per Well
	12-Well Plates	80 000 Per Well	40 000 Per Well
Immunocytochemistry	8-Chamber dishes	40 000 Per	20 000 Per
		Chamber	Chamber
Western Blotting	T25 Flasks	200 000 Per Flask	400 000 Per Flask
FACS	T75 Flasks	400 000 Per Flask	800 000 Per Flask

3.1.3 Curcumin treatment

Curcumin suspension was prepared directly before use by dissolving in 70% EtOH, stirring for 30 minutes and sterile filtering. Upon reaching 60% confluency, cells were treated with 0, 10, 50, 100 and 200 μ M Curcumin suspension and incubated at 37°C, 95% humidity and 5% CO₂ for 48h.

3.2 MTT assay

Cell viability was assessed via a modified (3-(4,5-Dimethylthiazol-2-yl)-2,5-diphenyltetrazolium bromide) (MTT) assay, as described by Gomez *et al* in 1997. The reduction of MTT into blue formazan pigment by viable mitochondria in healthy cells is exploited in this assay. Directly after curcumin treatment, medium was drained carefully and 750 μ l DPBS, warmed to 37°C, was slowly added to each well. 250 μ l MTT solution (0.01g/ml in DPBS, filtered before use) was then added to each well very carefully, plates were covered in foil and incubated at 37°C, 95% humidity and 5% CO₂ for 2h. After incubation, the MTT solution was drained off and 1 ml of 50:1 Isopropanol:Triton (1% Triton in Isopropanol containing 1% HCl) added to the wells.

In the case of cells loosening during the incubation step, the MTT solution was pipetted into centrifuge tubes and spun down for 2 minutes at 1000 rpm in a centrifuge. The supernatant was decanted and the previously mentioned 1 ml of 50:1 Isopropanol:Triton solution was added to the pellet. The pellet was gently resuspended and added back to the original well. Plates were then covered with foil and shaken for 5 minutes on a shaker. Cells were then transferred to centrifuge tubes and spun down for 2 minutes at 1400 rpm. The supernatant was decanted into cuvettes and the absorbance was read at 540 nm on a UV-Visible spectrophotometer, using the 50:1 Isopropanol:Triton solution as a blank.

3.3 Immunocytochemistry

3.3.1 Sample preparation

Staining was done in a darkened room to prevent premature fluorochrome bleaching; samples were stained directly after fixing to minimise background staining. Hoechst and propidium iodide (pi) staining was performed on the same samples. For pi and Hoechst staining, cells were grown on 16 mm round, autoclaved coverslips, previously placed into the wells of 12-well plates. For anti Beclin-1, -PARP, -LC3B and -Caspase-3 staining, cells were grown in 8-chamber dishes. After incubation with curcumin, cells were washed with DPBS before fixing for 10 minutes at 4 °C, on ice, with 500 µl of a 1:1 Methanol:Acetone solution per well (cells stained with pi were fixed after pi and before Hoechst staining). pi and Hoechst staining was done on the samples.

After fixing, the methanol:acetone solution was pipetted off and the plates left to air dry at room temperature for 20 minutes. One set of DPBS controls was prepared for

each set of antibodies used; the control receiving no primary antibody, but the same volume of diluted DPBS (1/10 dilution prepared with dH₂O; filtered before use; henceforth referred to as staining DPBS, or SDPBS. All antibodies, donkey serum, pi and Hoechst were diluted in SDPBS.

Air-dried coverslips were rinsed with DPBS and transferred to microscope slides in light protected humidified staining boxes. Each coverslip was then circled with a DAKO wax pen to prevent solutions draining off cells during incubation steps.

3.3.2 Propidium Iodide (PI)

PI was obtained from SIGMA, dissolved in PBS to a 5 mg/ml solution, aliquoted and stored at -20 °C. Aliquots were thawed on ice directly before staining and diluted with SDPBS to a 1:200 working solution. After coverslips were rinsed twice with SDPBS, 50 µl of the PI working solution was carefully pipetted onto the coverslip, taking care that the solution covered the entire coverslip. Thereafter, plates were incubated at 4°C for 20 minutes. Cells were then rinsed twice with SDPBS, and fixed. Slides were stained with Hoechst directly after fixing.

3.3.3 Hoechst

Hoechst 33342 was obtained from SIGMA, dissolved in PBS to a 10 mg/ml solution, aliquoted and stored at -20 °C. Aliquots were thawed on ice directly before staining and diluted with SDPBS to a 1:200 working solution. After coverslips were rinsed twice with SDPBS, 50 µl of the PI working solution was carefully pipetted onto the coverslip, taking care that the solution covered the entire coverslip. Thereafter, plates were incubated at 4°C for 20 minutes. Cells were then rinsed twice with SDPBS and remaining drops of SDPBS were carefully absorbed using a paper towel. Microscope

cover slides were then mounted onto the stained slides using UNIVAR glycerol. Slides were protected from light and stored at -20°C until analyzed for fluorescence.

3.3.4 Anti Beclin-1, -PARP, -LC3B and –Caspase-3

Table 3.2 Primary Antibodies used for Immunocytochemistry

<i>Antibody</i>	<i>Source</i>	<i>Dilution</i>	<i>Manufacturer</i>
Anti Caspase-3	Rabbit	1:50	Cell Signalling Technology
Anti PARP	Rabbit	1:50	Cell Signalling Technology
Anti LC3B	Mouse	1:50	Nano Tools
Anti Beclin-1	Rabbit	1:50	Assay Designs

Table 3.3 Secondary Antibodies used for Immunocytochemistry

<i>Antibody</i>	<i>Dilution</i>	<i>Manufacturer</i>
FITC-linked Donkey Anti Mouse	1:50	Vector Laboratories
Texas Red linked Donkey Anti Rabbit	1:50	Vector Laboratories

3.3.5 Immunocytochemistry procedures

A 30 minute blocking step was performed on fixed cells at room temperature, using 100 μ l of a 5% dilution of donkey serum (per slide), to block non-specific binding sites. After the blocking step, serum was drained off and 50 μ l of a 1:50 dilution of primary antibodies against Beclin-1, -PARP, -LC3B and -Caspase-3 were added to respective wells. Chamber dishes were covered with damp cloths, protected from light and incubated for 90 minutes at room temperature. Wells were then carefully washed twice with 200 μ l SDPBS per slide, before adding 50 μ l of a 1:200 dilution of secondary FITC or Texas Red-conjugated antibodies, directed against the animal species that the primary antibody was raised in. SDPBS control wells received both secondary antibodies. Diluted secondary antibodies were centrifuged briefly to allow crystals to collect at the bottom of the tube; only the supernatant was used for staining. Chamber dishes were again covered with damp cloths, protected from light and incubated for 30 minutes at room temperature. 50 μ l of a 1:200 dilution of Hoechst 3334 was then added and wells were incubated for another 10 minutes as described above. Wells were then drained and carefully washed twice with 200 μ l SDPBS per well, before adding one drop of Glycerol and analyzing for fluorescence.

3.4 Fluorescence Microscopy

3.4.1 PI and Hoechst

Images of stained cells were captured on a NIKON Eclipse E400 fluorescence microscope equipped with a NIKON DXM 1200 digital camera, using the NIKON ACT-1 program. 12 Images per DNA stain per time point for treated and untreated cells, respectively, were captured.

3.4.2 Anti Beclin-1, -PARP, -LC3B and –Caspase-3

Cells were observed on an Olympus Cell^AR system attached to an IX-81 inverted fluorescence microscope equipped with a F-view-II cooled CCD camera (Soft Imaging Systems). Z-stack image frames were acquired with a 0.26 µm step width, using an Olympus Plan Apo N 60x/1.4 Oil objective and the Cell^AR imaging software. Stack images were background subtracted and presented in a maximum intensity projection.

3.5 Fluorescence Activated Cell Sorting (FACS)

3.5.1 Sample preparation

Staining was done in a darkened room to prevent premature fluorochrome bleaching. Hoechst and Acridine Orange staining was performed on the same samples. Cells were cultured in T75 tissue culture treated flasks, and harvested and fixed directly after curcumin incubation. Cells destined for Hoechst staining were fixed in the following manner: Cells were trypsinized and transferred to 15 ml centrifuge tubes. Thorough, yet gentle pipetting was done with a 100 -1000 µl pipet to obtain a single cell suspension. Thereafter, cells were centrifuged for 5 minutes at 1000 g where after the supernatant was pipetted off carefully to prevent cell loss. The cell pellet was washed in this manner twice, with a cell count being performed before the last wash. After the last centrifugation step the supernatant was pipetted off carefully, and the pellet resuspended in 500 µl PBS – once again care was taken to obtain a single cell suspension. Hereafter 5 ml cold EtOH was added drop wise (to prevent clumping) while vortexing. Samples were stored at 4°C until stained.

Cells destined for Acridine Orange and CycleTEST™ PLUS staining, were fixed in the following manner: Cells were washed in PBS, diluted to 1×10^6 cells/ml and centrifuged at 200 g for 5 minutes. The cell pellet was then resuspended in 1 ml of PBS and fixed by incubating in 9 ml of 1% paraformaldehyde for 15 minutes, on ice. Cells were centrifuged at 200 g for 5 minutes, resuspended in 5 ml of PBS and centrifuged again. The pellet was then resuspended in 1 ml PBS and added to 9 ml 70% EtOH, on ice. Cells were incubated for 4 hours on ice at 4°C before storing at 4°C until stained.

3.5.2 Hoechst staining

Fixed cells were centrifuged at 200 g for 5 minutes and the supernatant was carefully pipetted off. The cell pellet was then vortexed and washed twice with 5 ml PBS + 0.1% bovine serum albumin (henceforth referred to as Staining Buffer). A cell count was done before the last wash, and cells diluted to 1×10^6 /ml Staining Buffer. An equal volume of 5 mM Hoechst 3334 in DMSO was added and incubated for 15 minutes at 37°C. Cells were protected from light and analyzed for fluorescence immediately after staining.

3.5.3 Acridine Orange staining

Fixed cells were centrifuged at 200 g for 5 minutes and the supernatant was carefully pipetted off. The pellet was resuspended in 200 µl PBS, before being incubated with 500 µl of 0.1M HCl at room temperature. After 30-45 seconds incubation, 2 ml of Acridine Orange staining solution was added; cells were protected from light, transferred to ice and immediately analyzed for fluorescence.

3.6. Methods of Protein Analysis

3.6.1 Bradford Protein Quantification

Samples were prepared for protein quantification by draining medium off cells directly after curcumin incubation and placing the flasks on ice. Cells were rinsed with cold PBS, where after 1ml RIPA buffer, pH 7.4, thawed previously on ice, was pipetted onto cells. After approximately 1 minute, a cell scraper was used to thoroughly scrape cells from the bottom of the flasks, and cells were transferred to microcentrifuge tubes with a pipette. Samples were then sonicated for 3-5 seconds at power level three, using a Vir Sonic 300, (Virtis Gardiner). Samples were kept on ice throughout the procedure. Samples were then centrifuged for 10 minutes at 4°C at 1000 x g in a ALC-PK121R centrifuge. A dilution series of 0, 2, 4, 8, 12, 16 en 20 µl protein was prepared by adding 0, 10, 20, 40, 60, 80 and 100 µl 1:4 BSA: dH₂O to 100, 90, 80, 60, 40, 20, and 0 µl dH₂O respectively in microcentrifuge tubes. Samples were prepared by adding 5 µl of each sample to 95 µl deionised water in microcentrifuge tubes. Tubes were then briefly vortexed, 900 µl Bradford working solution was added to each tube and briefly vortexed again. All samples were incubated at room temperature for 5 minutes, transferred to cuvettes, and the absorbance was read at a wavelength of 595 nm against the prepared blank of 100 µl dH₂O and 900 µl Bradford working solution. Absorbance was read twice per sample after which the weight of protein in µg/ml was plotted against absorbance and protein concentration was determined.

3.6.2 Sodium-dodecyl-sulfate-polyacrylamide gel electrophoresis (SDS-PAGE)

The previously calculated volume of sample buffer was added to microcentrifuge tubes in a fume cabinet; where after the correct volume of sample was added to each tube. One small hole was punched in the lid of each tube, where after samples were boiled for 5 minutes at 95° in a heating block. Samples were centrifuged for approximately 5 seconds in a centrifuge and stored at -80°C until protein separation with SDS-PAGE.

After a 10%, 1 mm separating gel was prepared a 4% stacking gel was poured on and 1 mm combs inserted. While setting, samples were thawed, briefly vortexed and boiled at 95°C for 5 minutes, before being briefly vortexed again. The Bio-Rad mini protean II™ gel loading system was assembled, running buffer poured into the compartment between the gel plates, and 7 µl of peqLab peqGOLD protein marker was added into the first well on the left of each gel. 20 µg Protein was loaded into each well, with Sample Buffer loaded into empty wells to prevent wells from bending during protein separation. The loading system was then placed into the outer running chamber, running buffer added, the system closed and the correct electrodes attached. An initial 10 minute run at 100V and 400 mA was performed to allow proteins to migrate from the stacking gel into the separating gel. Hereafter a ~50 minute run at 200V was performed.

Directly after protein separation, the gel was removed from the separating system for electrotransfer of proteins onto a polyvinylidene fluoride (PVDF) (Immobilon™ P, Millipore) membrane. Semi-dry transfer was performed in a BIO RAD trans-blot SD system. Eight pieces of chromatography/filter paper (Whatman Chr 3030917) were cut to the size of the gel, of which three were soaked in Anode Buffer 1 and placed

onto the anode plate. One paper was then soaked in Anode Buffer 2, and carefully placed on top of the other three papers. The paper stack was then rolled with a wet test tube to remove air bubbles. A piece of PVDF membrane cut to the size of the gel was then soaked in methanol for 15 seconds, rinsed in dH₂O, and then soaked in Anode Buffer 2. The membrane was placed onto the paper stack and rolled with a wet test tube to remove air bubbles. The gel was then carefully removed from between the glass plates of the loading system, placed onto the membrane and rolled with a wet test tube to remove air bubbles. Four papers were soaked in Cathode Buffer and placed onto the gel, after which the system was closed and a 60 minute run at 0.5 A and 15 V was performed. Hereafter, the membrane was washed in TBS-T (Tris Buffered Saline + 0.1% Tween 20) on a Labnet Gyro Twister for a total of 3 times for 5 minutes each.

A blocking step, consisting of incubating the membrane in 50 ml of 5% fat free powdered milk in TBS-T, on a shaker for 2 hours, was then performed. After blocking, the membrane was rinsed with TBS-T and incubated overnight on a DYNAL sample mixer at 4°C with the primary antibody of choice.

Table 3.4 Primary Antibodies Used For Protein detection

<i>Antibody</i>	<i>Source</i>	<i>Molecular Weight (kDa)</i>	<i>Dilution</i>	<i>Manufacturer</i>
Anti Caspase-3	Rabbit	17, 19, 35	1:1000	Cell Signalling Technology
Anti PARP	Rabbit	24, 89, 116	1:1000	Cell Signalling Technology
Anti Beclin-1	Rabbit	60	1:1250	Cell Signalling Technology
Anti β-Actin	Mouse	75	1:1000	Cell Signalling Technology

A KPL LumiGLO Reserve™ Chemiluminescent Substrate Kit was used for detection purposes. After incubation with primary antibody, the membrane was thoroughly washed with large volumes of Lumiglo Wash Solution on a Labnet Gyro Twister for a total of 3 times, 5 minutes each. Thereafter, the membrane was incubated for 60 minutes on a DYNAL sample mixer at room temperature with a 1:4000 dilution of HRP (Horseradish Peroxidase) conjugated secondary antibody (Amersham Life Sciences), directed against the species the primary antibody was raised in. After secondary antibody incubation, the membrane was thoroughly washed with TBS-T for a total of 3 times, 5 minutes each and thereafter incubated at room temperature for 5 minutes in Lumiglo detection reagents. Excess moisture was removed by dabbing the edges of the membrane on a paper towel, before transferring to an Amersham Biosciences Hypercasette™. The Membrane was exposed to an autoradiography film (Hyperfilm™) for a few seconds, before being developed and fixed in AXIM fixer and developer, all in a dark room.

Membranes were stripped by performing twice 5-minute washes in dH₂O, followed by one 5 minute wash in 0.2 M NaOH, followed by twice 5-minute washes in dH₂O. Thereafter membranes were reprobbed up to two times with alternate antibodies and exposed and developed as previously explained.

3.6.3 Film Analysis

Densitometry was done by firstly scanning films and thereafter analyzing it with UN-SCAN-IT, Silkscience software. Corrections were made for background noise.

3.7 Statistical methods

Results are presented as mean values \pm standard error of the mean (SEM). A one-way ANOVA (analysis of variance) with a Bonferroni type correction was performed, where a P-value of < 0.05 was considered as significant. All statistical analyses were conducted with the aid of GraphPadPRISM[®] version 4 software.

Chapter 4: Results

4.1 MTT

Dose response using 10-200 μ M curcumin in MCF-12A and MCF-7 cells

In order to investigate the effect of curcumin on the viability of MCF-7 and MCF-12A cells, a dose response over a time period of 48 hrs was performed. An MTT assay was executed after treating cells with 0, 10, 50, 100 and 200 μ M curcumin. No significant decrease in MCF-12A cell viability after curcumin treatment was found. However, the results indicate a significant decrease in MCF-7 cell viability when using 200 μ M curcumin [Mean \pm SEM% ($p < 0.05$)], compared to the control viability. A further significant drop in MCF-7 cell viability was seen between 10 and 200 μ M and 50 and 200 μ M treatment (Figure 4.1.2.).

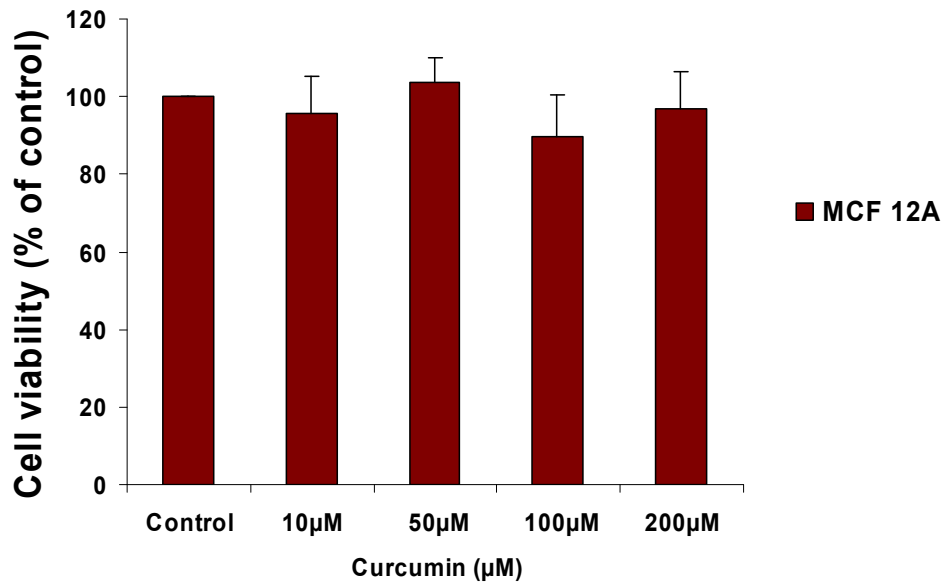


Figure 4.1.1 Viability in % showing control and treatment with curcumin of MCF-12A cells for a time period of 48 hrs using 10, 50, 100 and 200 µM concentrations, n = 9.

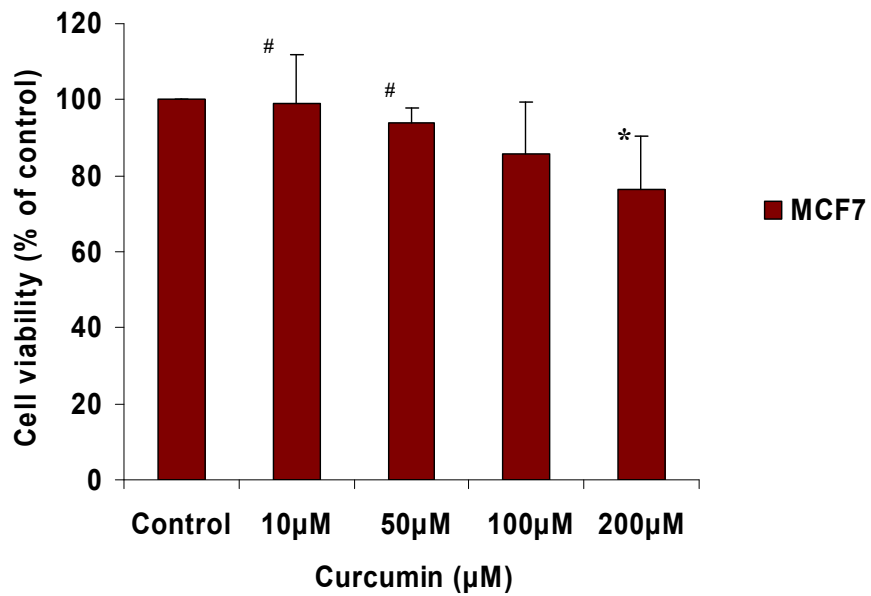


Figure 4.1.2 Viability in % showing control and treatment with curcumin of MCF-7 cells for a time period of 48 hrs using 10, 50, 100 and 200 µM concentrations. * $p < 0.05$ vs Control, # $p < 0.05$ vs 200 µM, $n = 9$.

4.2. Fluorescence Microscopy

4.2.1 Antibody staining

In order to investigate the expression of LC3, Beclin-1, Caspase-3 and PARP, immunocytochemistry was performed after treating MCF-12A and MCF-7 cells with 0, 10, 50, 100 and 200 μ M curcumin for 48 hrs. The nuclear stain Hoechst was employed to indicate the nuclear region. Except for a clear LC3 expression in treated MCF-7 cells, no other visible difference was noted between experimental groups.

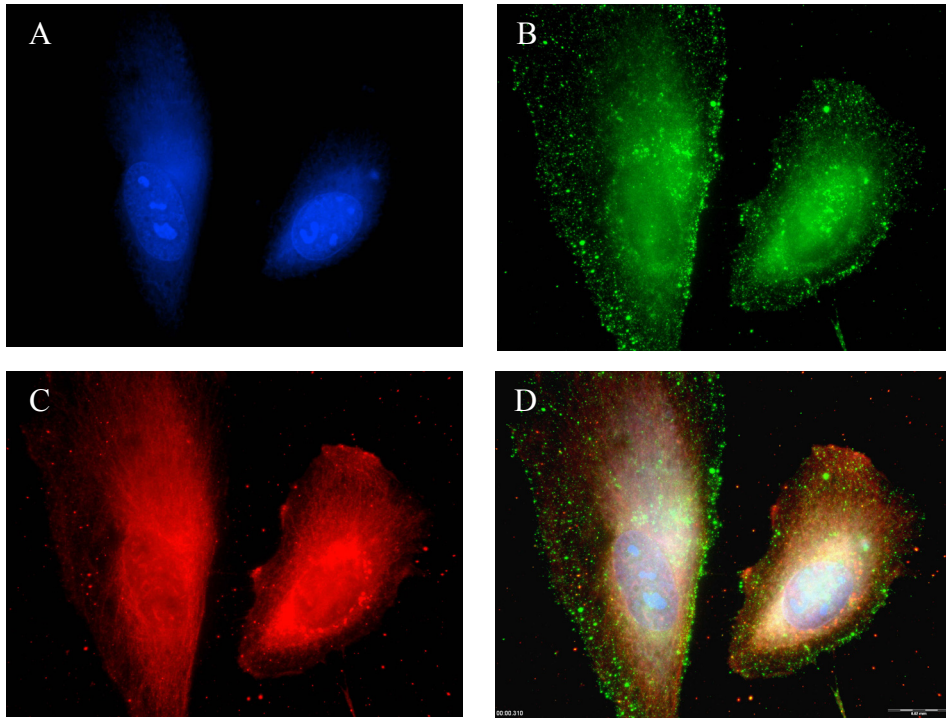


Figure 4.2.1.1 MCF-12A cells labelled with LC3/FITC displayed in green (B), Beclin/TexRed displayed in red (C), the nuclear indicator Hoechst, displayed in blue (A), and an image overlay (D). The figure shows MCF-12A cells untreated, n = 3.

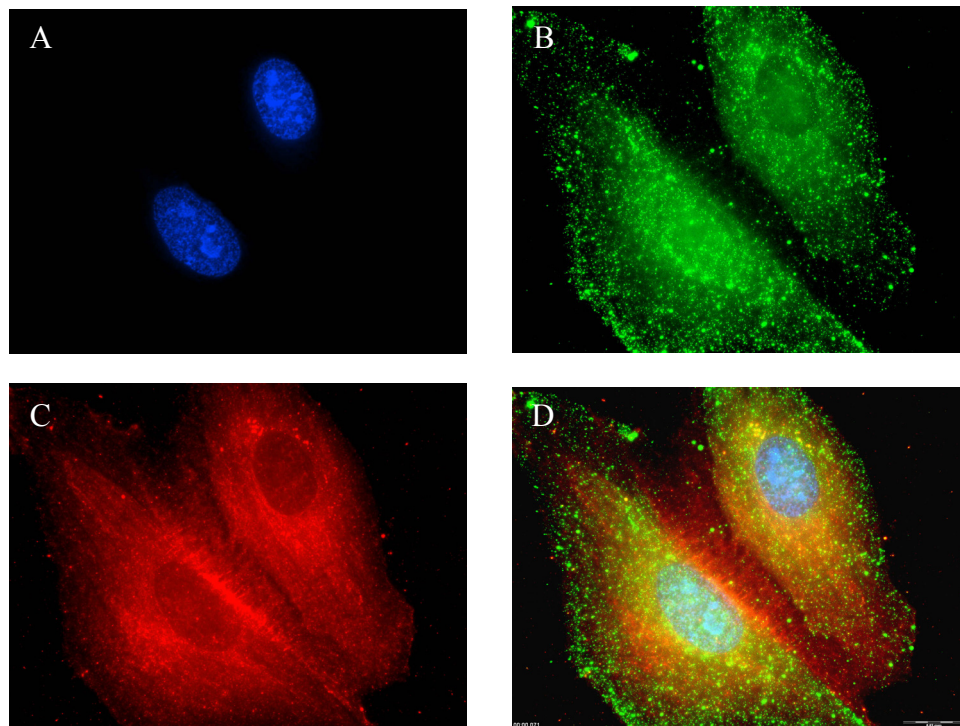


Figure 4.2.1.2 MCF-12A cells labelled with LC3/FITC displayed in green (B), Beclin/TexRed displayed in red (C), and the nuclear indicator Hoechst (A), displayed in blue, and an image overlay (D). The figure shows MCF-12A cells treated with 200 μ M curcumin, n = 3.

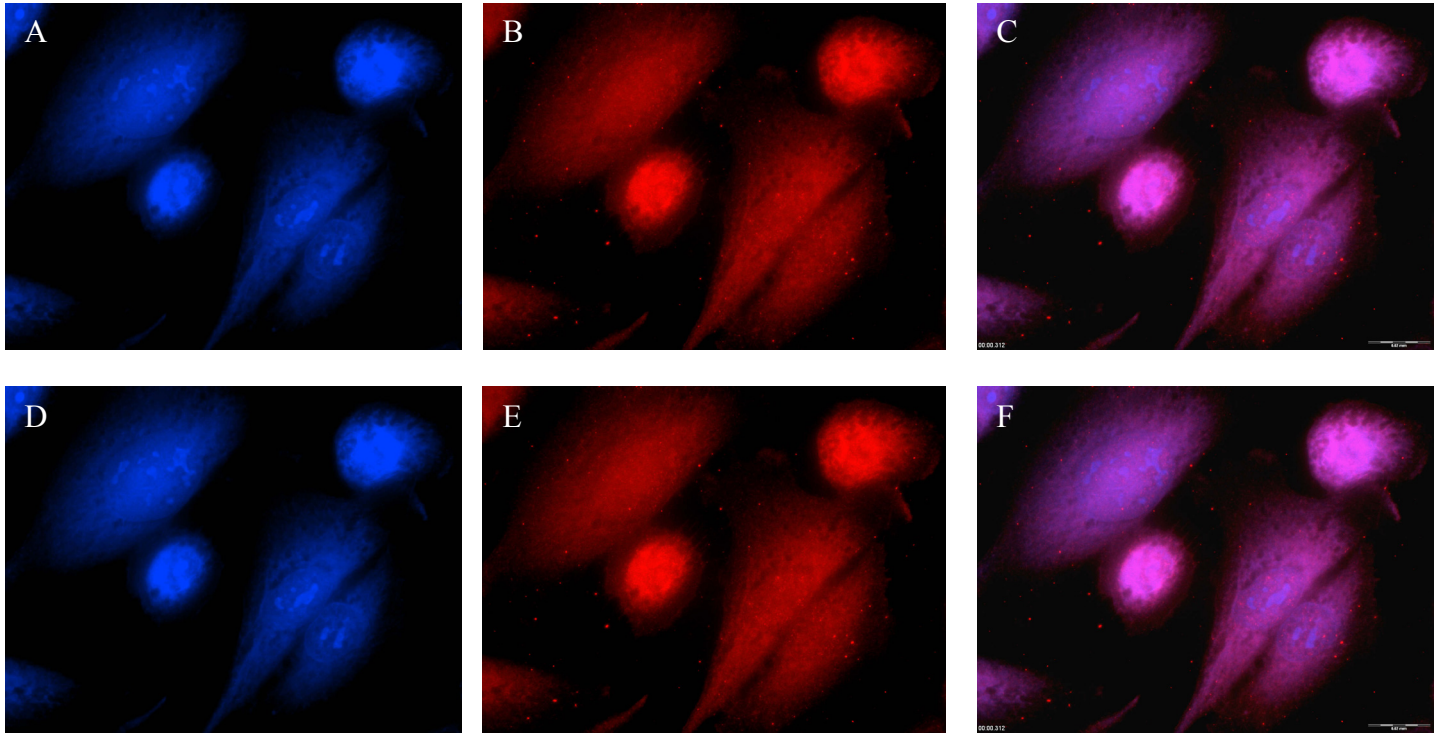


Figure 4.2.1.3 MCF-12A cells labelled with caspase-3/TexRed displayed in red , and the nuclear indicator Hoechst, displayed in blue. The figure shows MCF-12A cells untreated (A-C) and treated (D-F), n = 3.

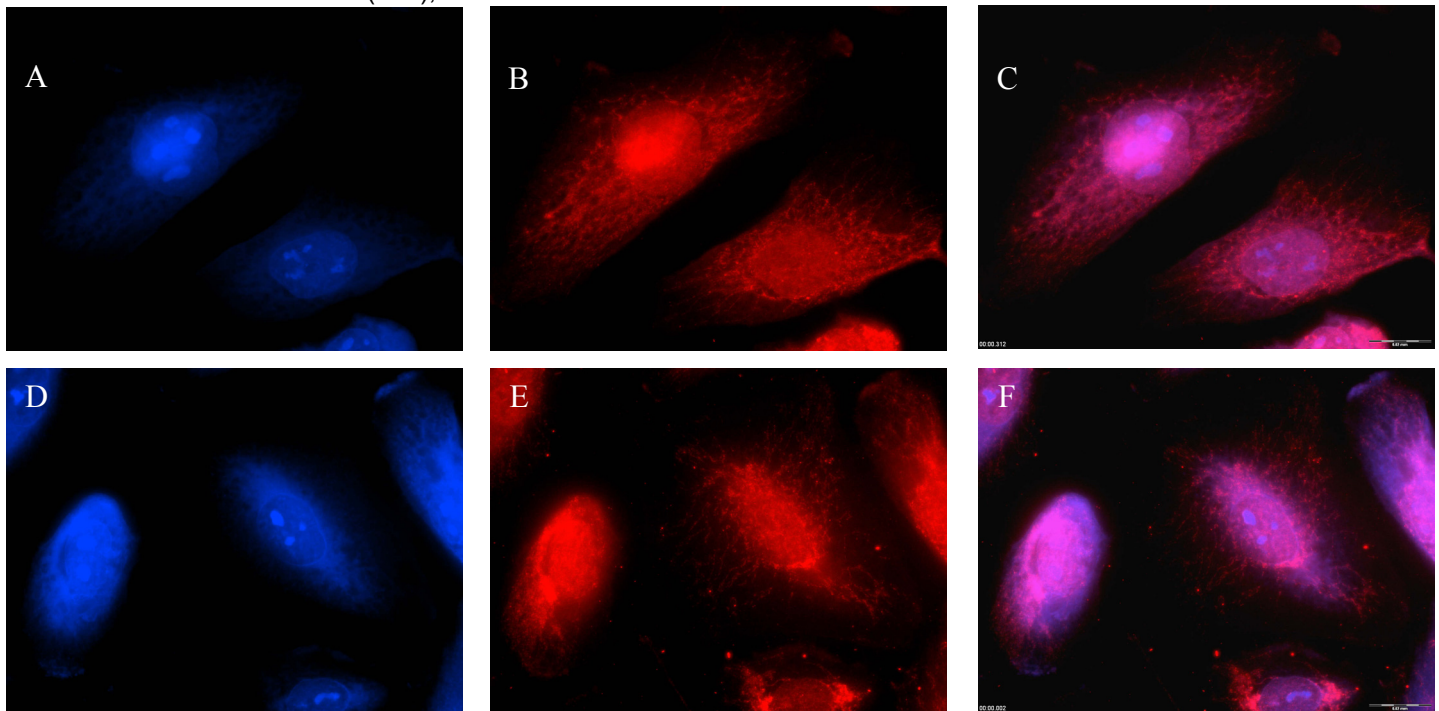


Figure 4.2.1.4 MCF-12A cells labelled with PARP/TexRed displayed in red and the nuclear indicator Hoechst, displayed in blue. The figure shows MCF-12A cells untreated (A-C) and treated (D-F), n = 3.

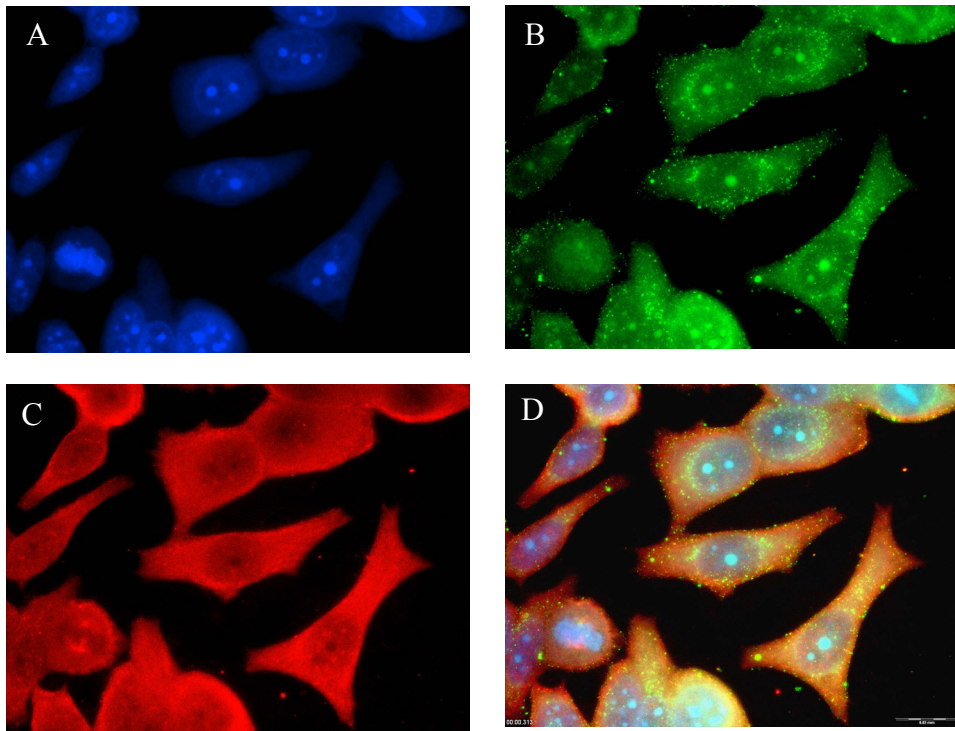


Figure 4.2.1.5 MCF-7 cells labelled with LC3/FITC displayed in green (B), Beclin/TexRed displayed in red (C), the nuclear indicator Hoechst, displayed in blue (A), and an image overlay (D). The figure shows MCF-7 cells untreated, n = 3.

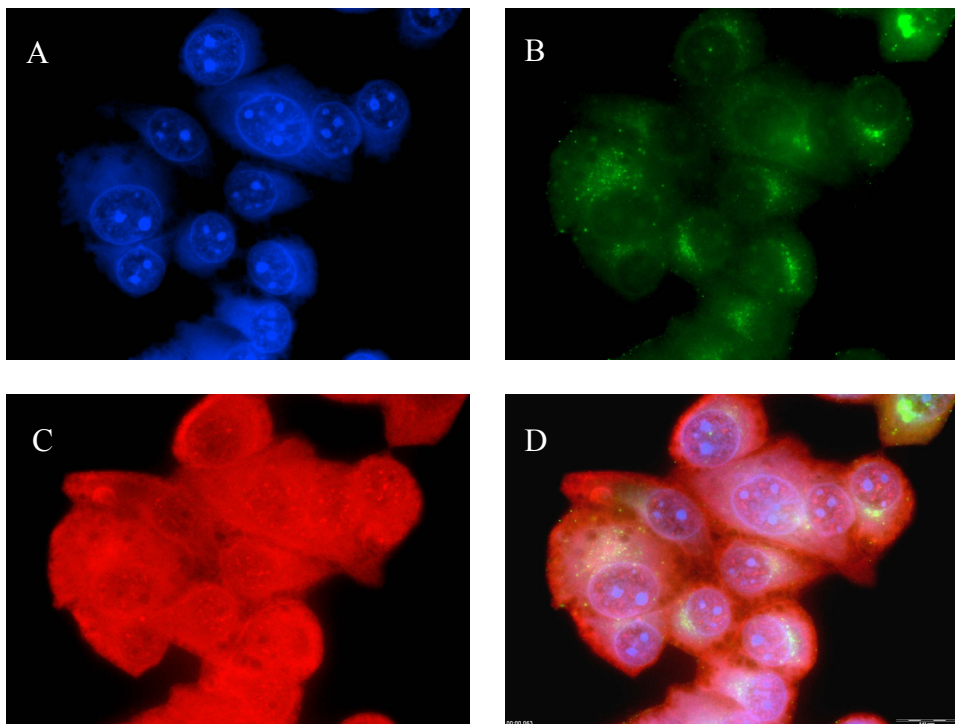


Figure 4.2.1.6 MCF-7 cells labeled with LC3/FITC displayed in green (B), Beclin/TexRed displayed in red (C), the nuclear indicator Hoechst, displayed in blue (A) and an image overlay (D). The figure shows MCF-7 cells treated, n = 3.

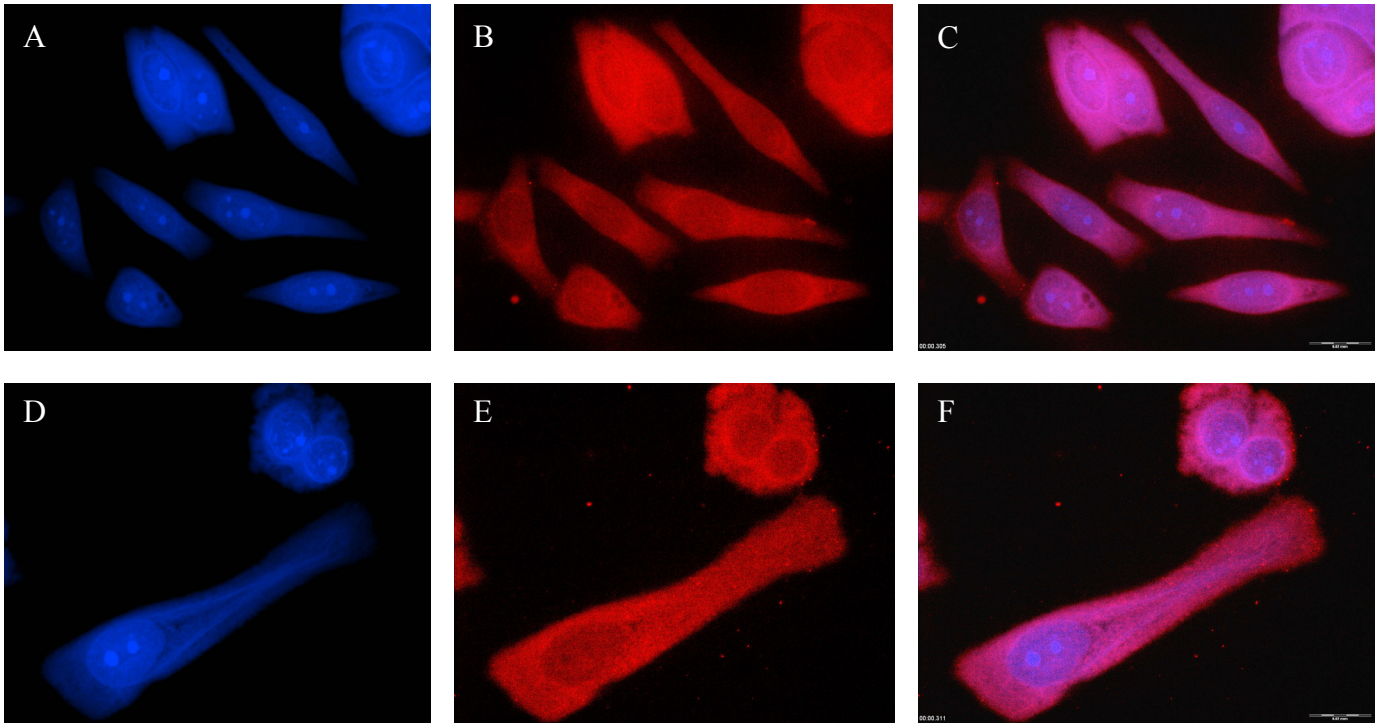


Figure 4.2.1.7 MCF-12A cells labelled caspase-3/TexRed displayed in red and the nuclear indicator Hoechst, displayed in blue. The figure shows MCF-12A cells untreated (A-C) and treated (D-F), n = 3.

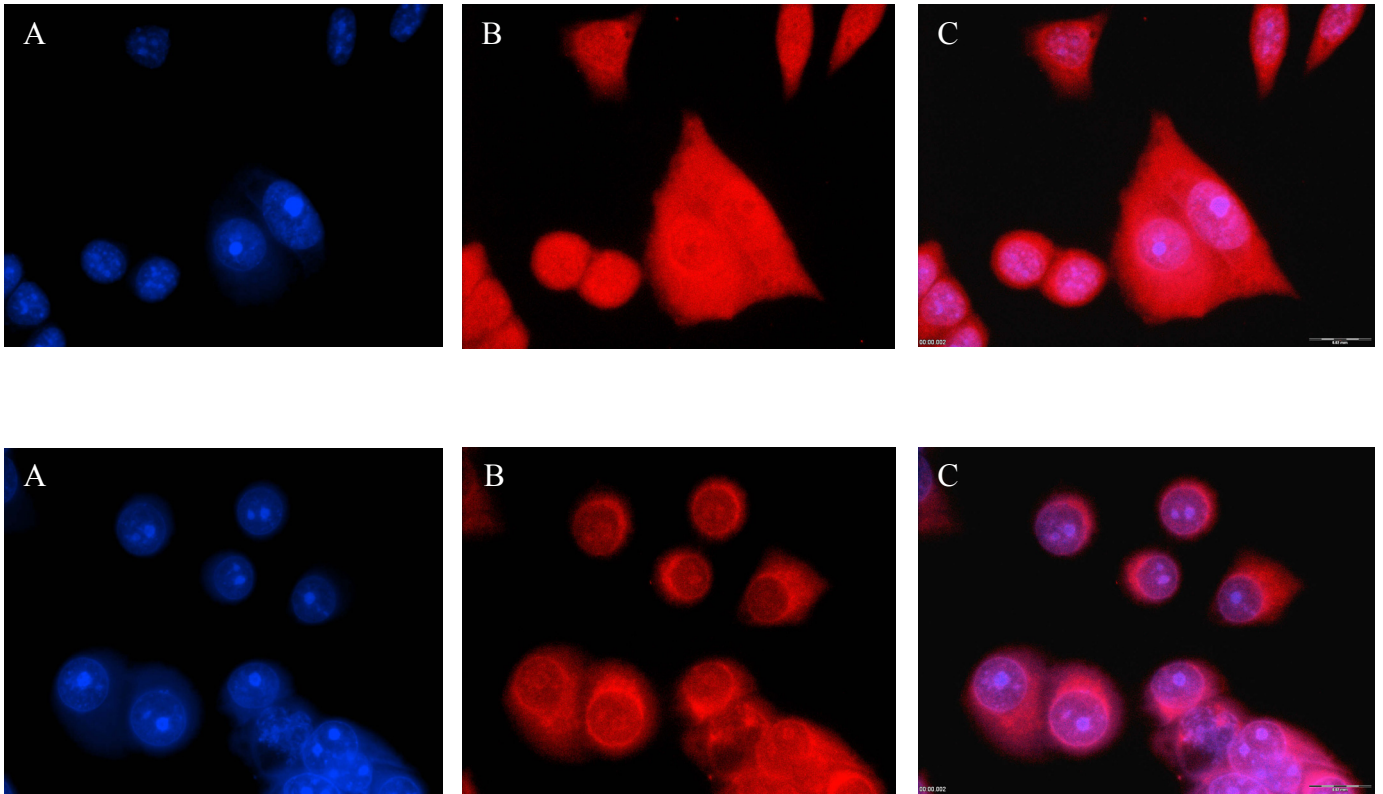


Figure 4.2.1.8 MCF-7 cells labelled with PARP/TexRed displayed in red and the nuclear indicator Hoechst, displayed in blue. The figure shows MCF-7 cells untreated (A-C) and treated (D-F), $n = 3$.

4.2.2. Propidium iodide exclusion technique

In order to assess the effect of the Curcumin treatment on membrane permeability, as indication for a leaking cell membrane and necrotic cell death, the propidium iodide exclusion method was performed. The results indicate that neither in the MCF-12A nor MCF-7 cells, a diffusion of propidium iodide into the cell was detected (Figure 4.2.2.1).

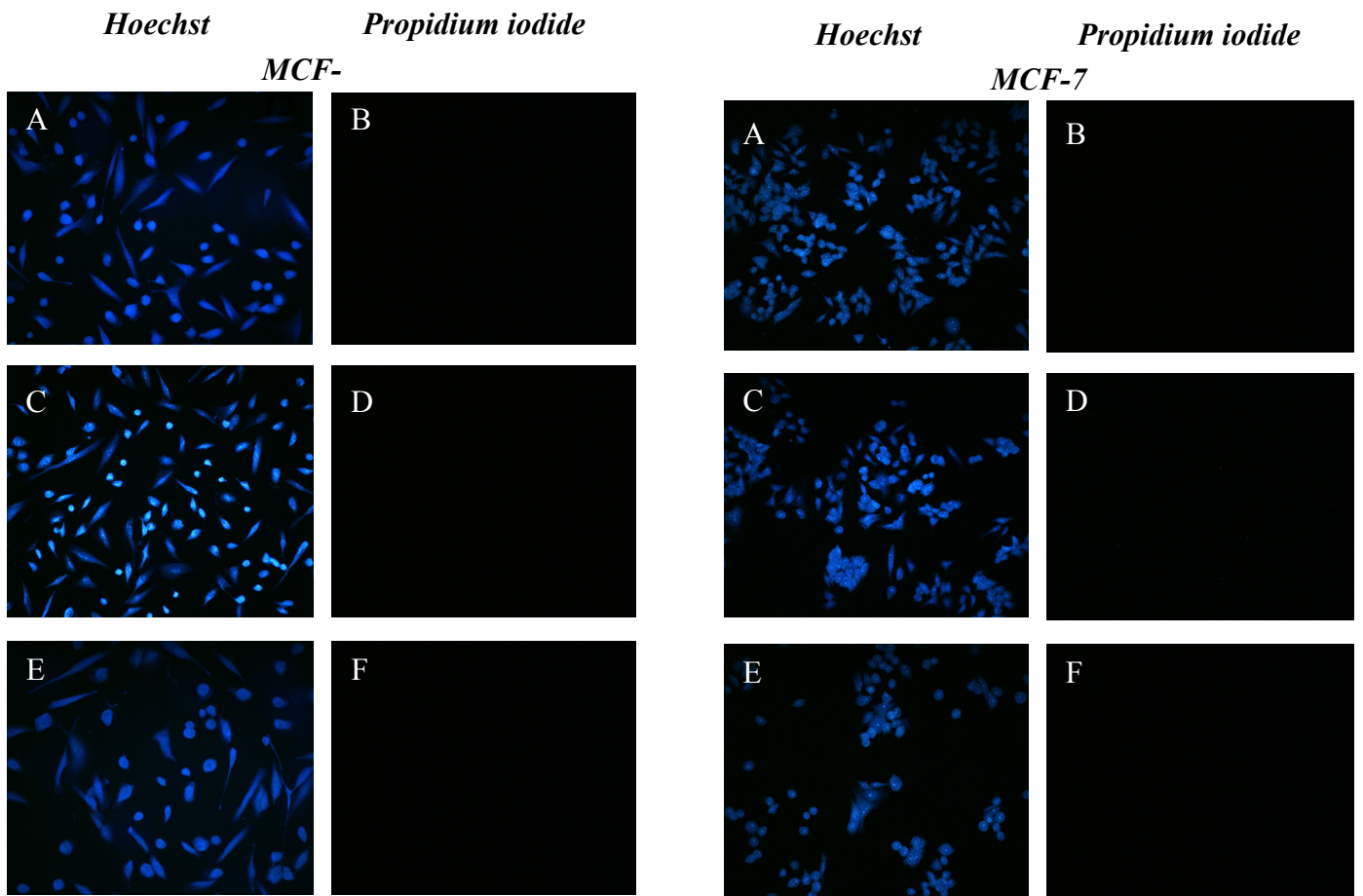


Figure 4.2.2.1 MCF-12A cells (left panel) and MCF-7 cells (right panel) incubated with Hoechst, displayed in blue, and Propidium iodide, displayed in red. Shown are untreated cells (A and B), vehicle controls (C and D) and treated cells (E and F), n = 3.

4.3 Western Blots

In order to evaluate Beclin-1, Caspase-3 and PARP expression, Western Blotting was performed after treating MCF-12A and MCF-7 cells with 0, 10, 50, 100 and 200 μ M curcumin for 48 hrs. No significant differences were observed in any of the groups.

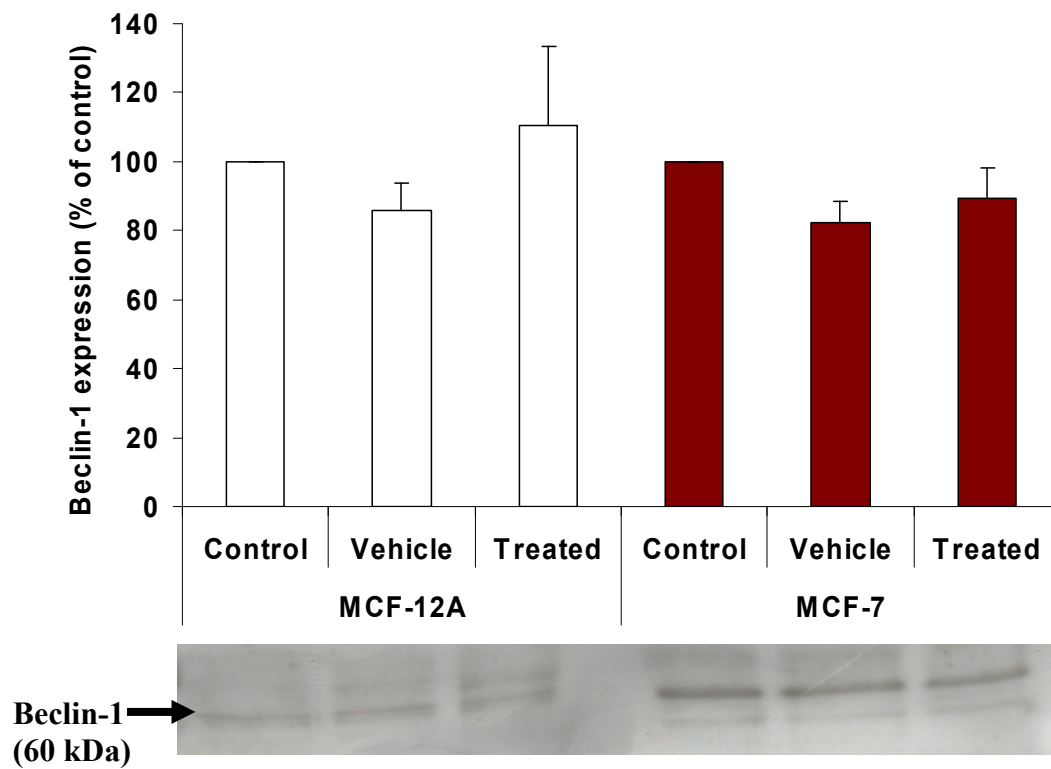


Figure 4.3.1 Schematic representation of Beclin-1 expression, in % of control in MCF-12A and MCF-7 cells, after no treatment, vehicle treatment, or treatment with 200 μ M curcumin, all for 48 hrs, n = 3.

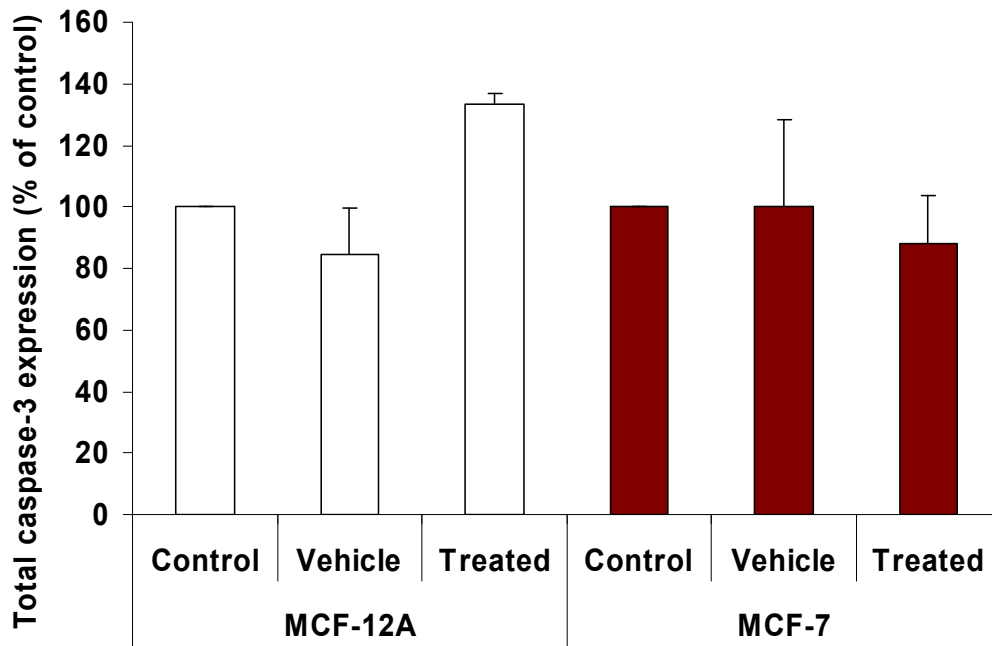


Figure 4.3.2 Schematic representation of total caspase-3 expression, in % of control in MCF-12A and MCF-7 cells, after no treatment, vehicle treatment, or treatment with 200 μ M curcumin, all for 48 hrs, n = 3.

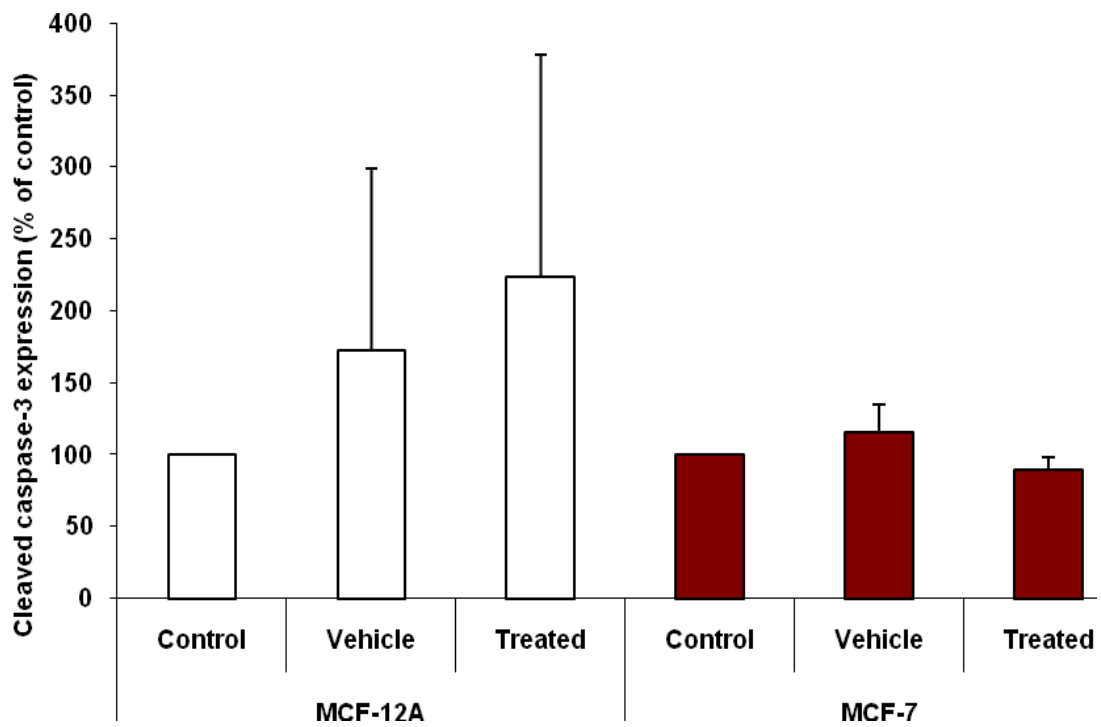


Figure 4.3.3 Schematic representation of cleaved caspase-3 expression, in % of control in MCF-12A and MCF-7 cells, after no treatment, vehicle treatment, or treatment with 200 μ M curcumin, all for 48 hrs, n = 3.

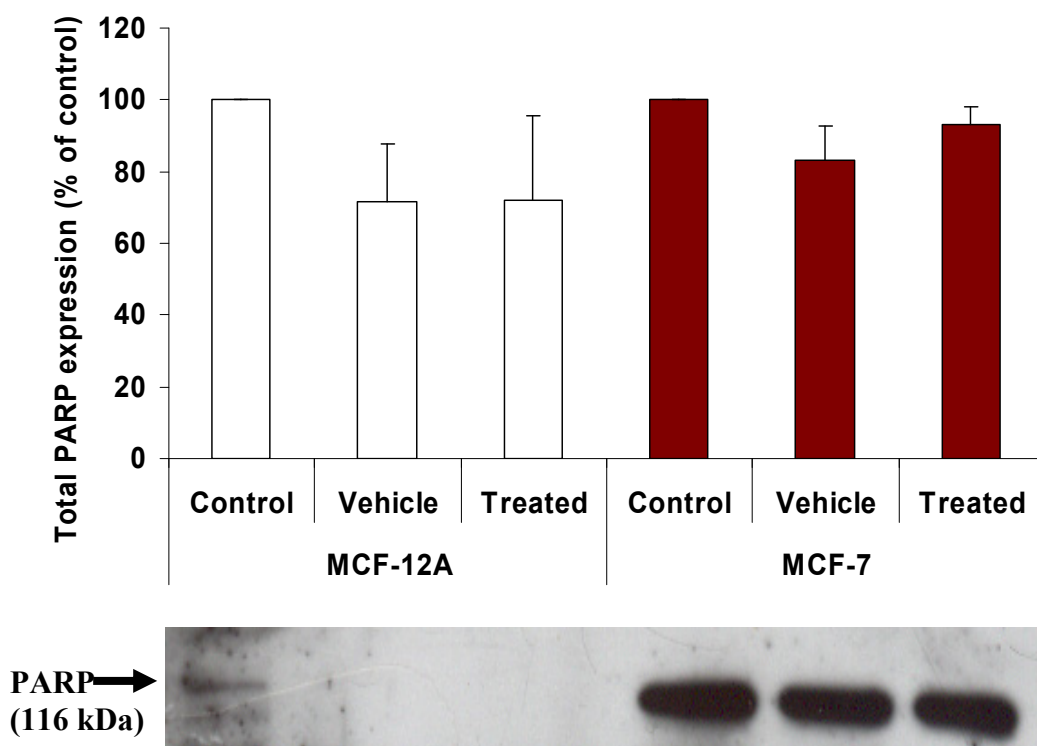


Figure 4.3.4 Schematic representation of Total PARP expression, in % of control in MCF-12A and MCF-7 cells, after no treatment, vehicle treatment, or treatment with 200 μ M curcumin, all for 48 hrs, n = 3.

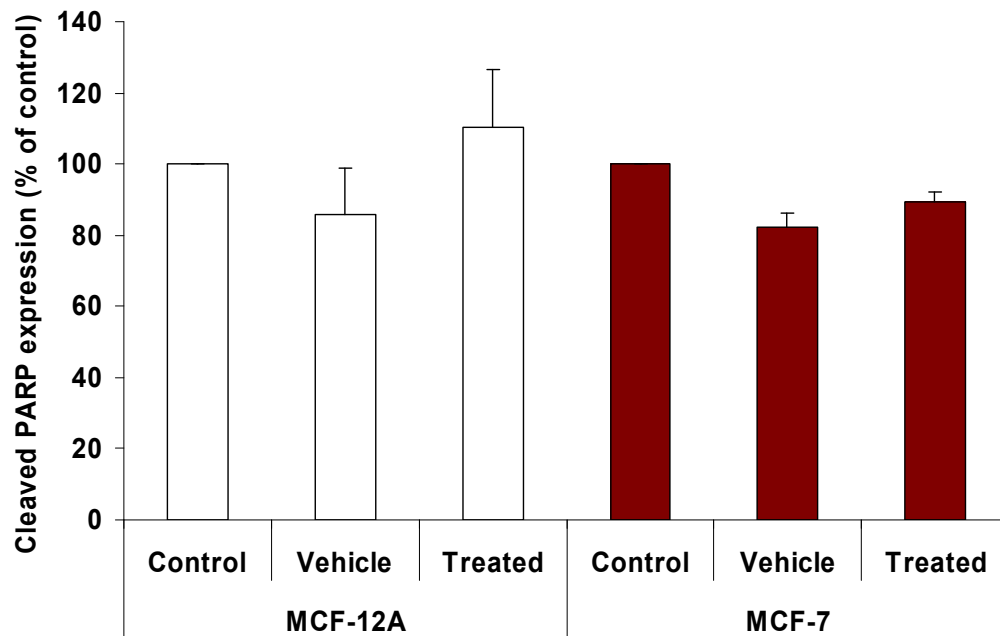


Figure 4.3.5 Schematic representation of cleaved PARP expression, in % of control in MCF-12A and MCF-7 cells, after no treatment, vehicle treatment, or treatment with 200 μ M curcumin, all for 48 hrs, n = 3.

4.4 Flow cytometry:

4.4.1 Acridine orange staining

In order to assess Acridine orange mean fluorescence intensity, MCF-12A and MCF-7 cells were stained with Acridine orange, after treatment with 0, 10, 50, 100 and 200 μ M curcumin for 48 hrs. In both groups, a significant decrease is seen in mean fluorescence intensity between control and 200 μ M treated groups, and between vehicle and 200 μ M groups.

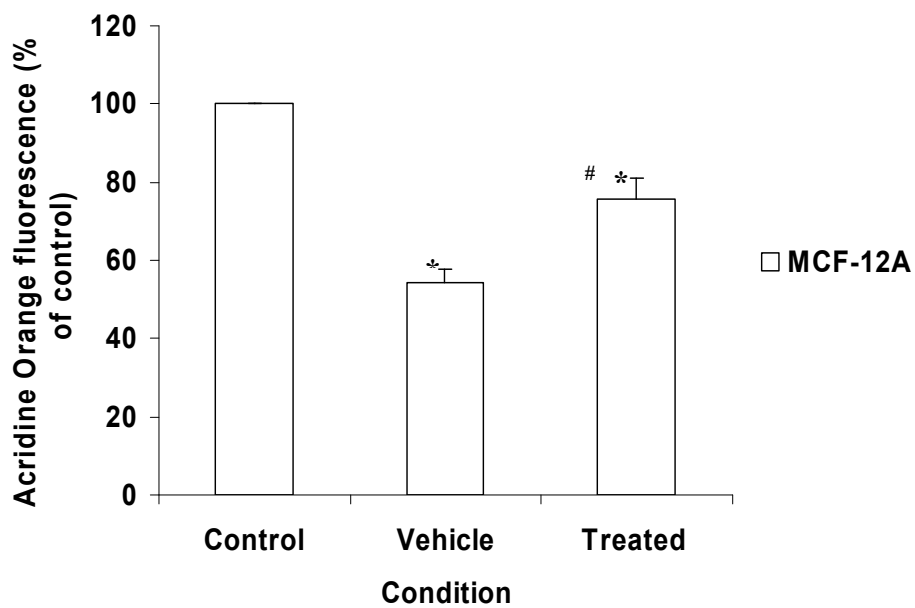


Figure 4.4.1.1 Acridine orange mean fluorescence intensity presented as a % of the control in MCF-12A cells, after no treatment, vehicle treatment, or treatment with 200 μ M curcumin, all for 48 hrs. * $p < 0.05$ vs Control, # $p < 0.05$ vs vehicle, $n = 3$.

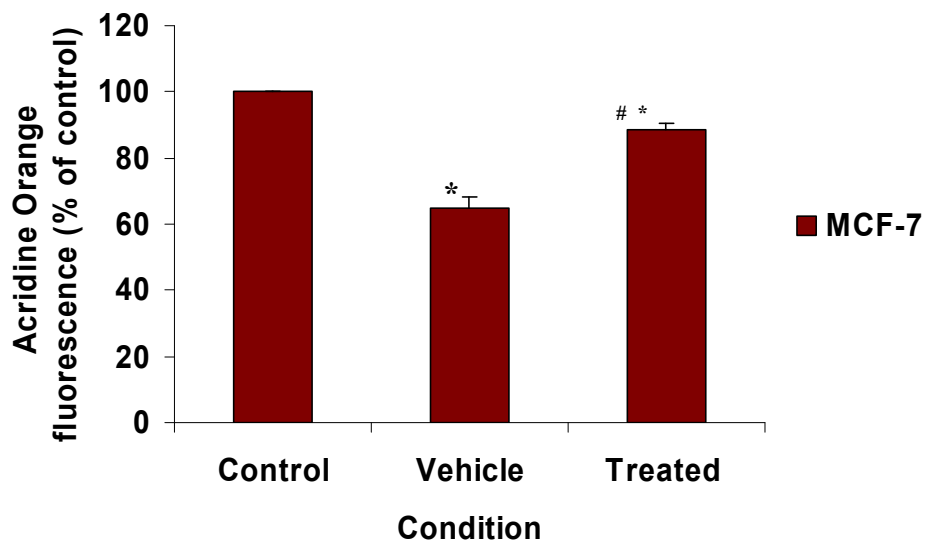


Figure 4.4.1.2 Acridine orange mean fluorescence intensity presented as a % of the control in MCF-7 cells, after no treatment, vehicle treatment, or treatment with 200 μ M curcumin, all for 48 hrs. * $p < 0.05$ vs Control, # $p < 0.05$ vs vehicle, $n = 3$.

4.4.2 Hoechst staining

In order to assess Hoechst mean fluorescence intensity, MCF-12A and MCF-7 cells were stained with Hoechst, after treatment with 0, 10, 50, 100 and 200 μM curcumin for 48 hrs. In both groups, a significant decrease is seen in mean fluorescence intensity between control and 200 μM treated groups, and between vehicle and 200 μM groups.

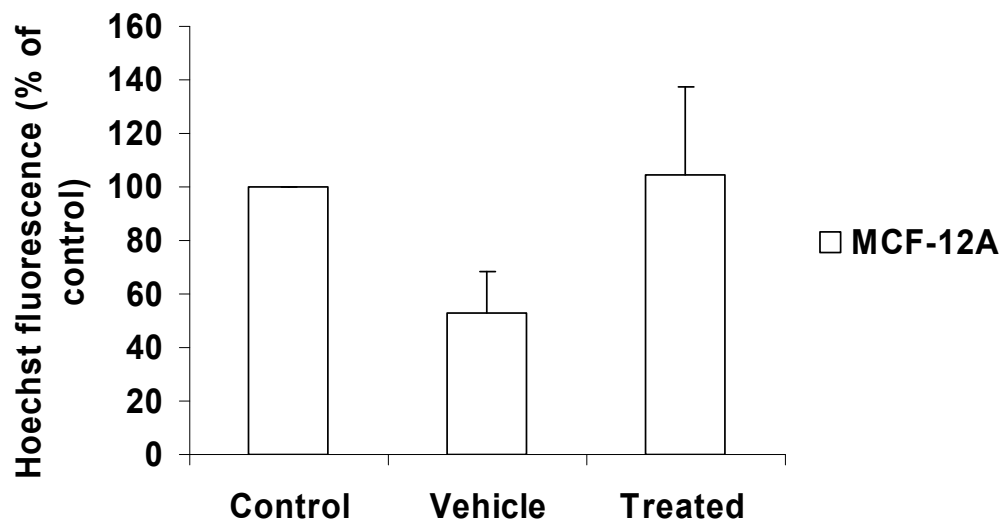


Figure 4.4.2.1 Hoechst mean fluorescence intensity presented as a % of the control in MCF-12A cells, after no treatment, vehicle treatment, or treatment with 200 μ M curcumin, all for 48 hrs.

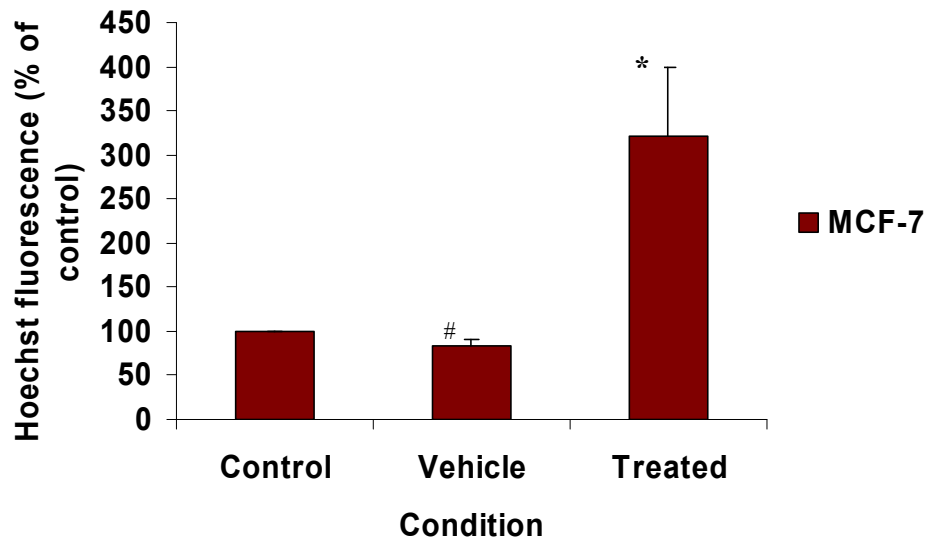


Figure 4.4.2.2 Hoechst mean fluorescence intensity presented as a % of the control in MCF-12A cells, after no treatment, vehicle treatment, or treatment with 200 μ M curcumin, all for 48 hrs. * $p < 0.05$ vs Control, # $p < 0.05$ vs 200 μ M.

Chapter 5: Discussion and conclusions

Curcumin has long been implicated in the modulation of several targets that have been linked to neoplastic, neurological, cardiovascular, pulmonary and metabolic illnesses. Due to the key role of inflammation in most chronic maladies, the interest lies particularly in the fact that curcumin exhibits anti-inflammatory properties (Aggarwal & Sung, 2008). Subsequent research has shown that it mediates this effect through down regulation of inflammatory enzymes (such as cyclooxygenase 2 and 5-lipoxygenase), transcription factors (for instance nuclear factor κ B) and cytokines (for example tumour necrosis factor and interleukins 1 and 6). The molecular properties that are believed to lend to curcumin its antiproliferative and anti-inflammatory effects, are the presence of bis- α,β -unsaturated β -diketone, two methoxy groups, two phenolic hydroxy groups and two double-conjugated bonds (Fig. 2.1.) (Aggarwal & Sung, 2008). Curcumin either binds directly to the target and modulates the activity, or has an indirect effect via consequent up- or down regulation of the target (Aggarwal & Sung, 2008). Curcumin has also been shown to impede proliferation and survival of most types of tumour cells studied to present. This effect is exerted via down regulation of AP-1, cyclins D1 and E, and upregulation of p21, p27 and p53 (Goel *et al.*, 2008). Tumour cells also showed lower glutathione levels than normal cells, rendering the tumour cells more sensitive to curcumin treatment (Syng-Ai, 2004). Most tumour cells also express constitutively active NF- κ B which mediates their survival (Shishoda *et al.*, 2005). In addition, Garg *et al.*, (2005) have shown that curcumin acts as a powerful chemo- and radio-sensitizer against tumour cells, via the down regulation of NF- κ B and NF- κ B-regulated gene products.

A major limitation of curcumin treatment studies is the poor bioavailability when administered orally (Anand *et al.*, 2007). In studies done on rodents and humans, very low or nil curcumin metabolites was found in serum or tissue following treatment (Garcea *et al.*, 2005; Ireson *et al.*, 2002). Various approaches have since been taken to augment the bioavailability, which involve: a) the use of an adjuvant such as piperine, interfering with glucuronidation; b) the use of liposomal curcumin; c) employing curcumin nanoparticles; d) the use of a curcumin-phospholipid complex, and e) the use of structural analogs of curcumin. In a study done on rats, the use of piperine combined with curcumin showed an increase in the serum concentration 1-2 hrs post treatment, and a 154% increase in bioavailability (Shoba *et al.*, 1998). In another study, a curcumin-piperine combination was administered to humans, where much higher serum levels and a 2000 % increase in bioavailability was observed, compared to administering of curcumin alone. Both the rat and human subjects experienced no adverse effects.

The present study was undertaken to evaluate the chemopreventative-/antiproliferative potential of curcumin on a breast cancer cell line and to investigate the different types of cell death which were induced, namely apoptosis, necrosis and autophagy. Treatment with curcumin (200 μ M for 48h) resulted in a significant decrease in the viability of cancer cells (MCF-7) while the viability of the normal cells (MCF-12A) was unaffected.

The MTT assay which was used to assess viability is based upon the following principle: the reduction of MTT to blue formazan is catalyzed by mitochondrial dehydrogenases, and the intensity of MTT staining is therefore indicative of mitochondrial activity. The significant decrease in viability which was demonstrated

with 200 μM curcumin treatment in the MCF-7 cell line is indicative of decreased mitochondrial activity in response to cell stress induced by curcumin (Niv *et al.*, 2005). No significant decrease in viability was observed when cells were incubated with the lower concentrations (10 μM , 50 μM and 100 μM) of curcumin. This is in contrast with the results obtained by Weir and co-workers (2007) who reported that concentrations as low as 10-50 μM of curcumin inhibited cell proliferation in a dose-dependent manner in an ovarian cancer cell line. This discrepancy may be due to differences in the model used, since the duration of the incubation period with curcumin was 48 h in both of the studies.

In order to assess the induction of autophagy and autophagic cell death, cells were stained after treatment with fluorochromes linked to anti-LC3 and -Beclin-1 antibodies. Treated MCF-7 cells respond to curcumin through the autophagic pathway, as microscope images showed clear changes in localization of LC3, manifesting as autophagic vesicles in a bright, punctuate pattern, which is indicative of an induction of autophagy. Treated MCF-12A cells did not show localization of LC3 in this manner. The autophagy-promoting activity of beclin-1 in MCF-7 cells is usually associated with inhibition of MCF-7 cellular proliferation and tumorigenesis in nude mice. Furthermore, endogenous beclin-1 protein expression is frequently low in human breast epithelial carcinoma cell lines and tissue, but is expressed ubiquitously at high levels in normal breast epithelia (Liang *et al.*, 1999). This is in contrast to our results where no significant differences were observed in beclin-1 expression between untreated and treated cells in both cell lines. This was also confirmed by western blot data where no changes in beclin-1 expression were observed. There

were also no significant differences in beclin-1 expression between the MCF-12A and MCF-7 cell lines.

Another marker for autophagy, acridine orange, was utilized in this study. Both cell lines showed a significant decrease in acridine orange mean fluorescence intensity after curcumin treatment. This is in contrast with results reported by Katz and co-workers who reported increased lysosomal activity after curcumin treatment in cancer cells (Katz *et al.*, 1985). It may be that a change is introduced into lysosomal compartmental arrangement, but that needs to be further investigated. Also, a possible explanation for this decreased expression could be that the dye is rapidly fluxed out by the cells after uptake. However, this concept calls for further investigation.

Various methods were used to assess apoptosis in the MCF-12A and MCF-7 cell lines after curcumin treatment. Hoechst nuclear stains revealed no significant differences in nuclear condensation or in formation of apoptotic bodies in microscope images in both cell lines. However, FACS analysis does show an increase in Hoechst mean fluorescence intensity. This could indicate a manifestation of early apoptosis, but the notion is ruled out by a lack of significant expression of caspase-3 and PARP in corresponding western blots. Also, when taking into consideration the chronological order of the apoptosis cascade, especially the fact that caspase-3 and PARP cleavage takes place upstream of induction of nuclear condensation and fragmentation, the possibility exists that the cells are in the earlier stages of apoptosis.

Hallmarks of necrosis include karyolysis, pyknosis and karyorrhexis, chromatin condensation and severe cytoplasmic eosinophilia. Furthermore, breakdown of the

plasma membrane and compromised membrane integrity is followed by the introduction of inflammation around the cell (Majno & Joris, 1995). PI exclusion results show no indication of membrane integrity changes in both the MCF-12A and MCF-7 cell lines, and thus no indication for necrosis. This is beneficial in our model, since disruption of the plasma membrane that is characteristic of necrotic cell death leads to spillage of intracellular proteins that activates a damage response from the host immune system (Festjens *et al.*, 2006).

Conclusions

The results of this study confirmed a definite response on a metabolic, but not on a cell death level, in MCF-7 cells to treatment with 200 μ M curcumin. This possible stress response manifests as a decrease in mitochondrial capacity. It can thus be concluded that curcumin definitely acts as a metabolic stressor of MCF-7 cells by increasing autophagy through the re-localization of LC3 vacuoles. However, neither apoptotic nor necrotic phenotypes were observed in our cell model as indicated by fluorescence microscopy. Although the MTT results clearly showed a decrease in viability in MCF-7 cells on mitochondrial level, it cannot be ruled out that apoptosis or necrosis could still be induced if the incubation period was prolonged or if a higher concentration of curcumin was used. Thus, it can be concluded from the results that autophagy is initiated as a result of the cellular stress induced by curcumin in MCF-7 cells. However, we can only speculate about apoptosis, since no markers of this type of cell death were observed. Frequently autophagy occurs before, but independently of apoptosis. This ordered sequence of autophagy and apoptosis may serve either of two purposes: first, autophagy may constitute a mechanism through which the cell destined to die initiates its catabolism, thus accelerating the disappearance of the cell

or secondly, autophagy may also help to maintain optimal high ATP levels that may facilitate the apoptotic process.

Advantages and disadvantages of this model

The use of a cell line based tissue culture model permits the convenience of a controlled environment, suitable to study molecular mechanisms. Also, with cells growing in a monolayer, an equal diffusion gradient is achieved. It greatly limits influencing factors such as decreased bioavailability which is observed in *in vivo* models.

However, care must be taken when this basic knowledge is translated into clinical practice as the physiological relevance of a cell culture model will always be questioned as multiple cell types, blood supply and the immune response of *in vivo* situations are not accounted for.

Future directions

Future work could include more time points of incubation of cells with curcumin to establish an optimal time necessary to induce cell death. Following this up with MTT assays as well as with Hoechst and PI staining would show whether cells recover from a temporal downregulation of general metabolic activity or if cell death was indeed induced. Other metabolic parameters such as AMPK, and mTOR could also be employed in addition to an MTT assay to establish their role in cell death. Earlier markers of apoptosis such as annexin v should be used to clarify if apoptosis is induced when no later events in the apoptotic cascade are observed. These results could be further investigated by repeating the experiments with an increased sample

size, and subsequently viewing cells microscopically to confirm the quantity of lysosomal areas after acridine orange staining.

The prevention and treatment of cancer remains a challenge as only a few drug therapies have demonstrated to be successful in reducing the mortality rate in cancer patients. Dietary intake of modest amounts of curcumin in patients as a preventative or treatment measure is a low-cost, low-risk intervention. It is time for clinicians, researchers and policymakers to give increased attention to the beneficial effects of these phytochemicals and to translate this considerable body of evidence into clinical practice.

References

- ADAMS, J.M., CORY, S. (1998). The Bcl-2 protein family: arbiters of cell survival. *Science*, **281 (5381)**:1322-1326.
- ADAMS, J., KAUFFMAN, M. (2004). Development of the proteasome inhibitor Velcade (Bortezomib). *Cancer Invest*, **22 (2)**: 304–11.
- AGGARWAL, B.B., KUMAR, A., BHARTI, A.C. (2003). Anticancer potential of curcumin: Preclinical studies. *Anticancer Res*, **23**: 363-398.
- AGGARWAL, B.B., SUNG B. (2008). Pharmacological basis for the role of curcumin in chronic diseases: An age-old spice with modern targets. *Trends Pharmacol Sc* [Epub ahead of print].
- AGGARWAL, S., TAKADA, Y., SINGH, S., MYERS, J. N., AGGARWAL, B. B. (2004). Inhibition of growth and survival of human head and neck squamous cell carcinoma cells by curcumin via modulation of nuclear factor-kappaB signalling. *Int J Cancer*, **111**: 679–692.
- ANAND, P., *et al.* (2007). Bioavailability of Curcumin: Problems and promises. *Mol Pharm*, **4**: 807-818.
- AOIKI, H., TAKADA, Y., KONDO, S., SAWAYA, R., AGGARWAL, B.B., KONDO, Y. (2007). Evidence that Curcumin suppresses the growth of malignant gliomas in vitro and in vivo through induction of autophagy: Role of Akt and extracellular signal-regulated kinase signalling pathways. *Mol Pharmacol*, **72**: 29-39.
- ARITOMI M., KUNISHIMA N., INOHARA N., ISHIBASHI Y., OHTA S., MORIKAWA K. (1997). Crystal structure of rat Bcl-xL. Implications for the function of the Bcl-2 protein family. *J Biol Chem*, **272 (44)**:27886-27892.
- BALSARA, B.R., PEI, J., DE RIENZO, A., SIMON, D., TOSOLINI, A., LU, Y.Y., SHEN, F.M., FAN, X., LIN, W.Y., BUETOW, K.H., LONDON, W.T., TESTA, J.R. (2001). Human hepatocellular carcinoma is characterized by a highly consistent pattern of genomic imbalances, including frequent loss of 16q23. *Genes Chromosomes Cancer*, **30**: 245-253.
- BANDO, K., NAGAI, H., MATSUMOTO, S., KOYAMA, M., KAWAMURA, N., TAIJIRI T., ONDA, M., EMI, M. (2000). Identification of a 1-Mb common region at 16q24.1-24.2 deleted in hepatocellular carcinoma. *Genes Chromosomes Cancer*, **28**: 38-44.
- BELAKAVADI, M., SALIMATH, B.P. (2005). Mechanism of inhibition of ascites tumor growth in mice by curcumin is mediated by NF-kB and caspase activated DNase. *Mol Cell Biochem*, **273**: 57–67.

- BOULARES, A.H., YAKOVLEV, A.G., IVANOVA, V., STOICA, B.A., WANG, G., IYER, S., SMULSON, M. (1999). Role of poly(ADP-ribose) polymerase (PARP) cleavage in apoptosis. *J Biol Chem*, **274**: 22932-22940.
- BURDALL, S.E., HANBY, A.M., LANSDOWN, M.R.J., SPEIRS, V. (2003). Breast cancer cell lines: friend or foe? *Breast Canc Res*, **5**: 89-95.
- BUSH, J. A., CHEUNG, K. J., JR., LI, G. (2001). Curcumin induces apoptosis in human melanoma cells through a Fas receptor/caspase-8 pathway independent of p53. *Exp Cell Res*, **271**: 305 –314.
- CANDÉ, C., COHEN, I., DAUGAS, E., RAVAGNAN, L., LAROCLETTE, N., ZAMZAMI, N., KROEMER, G. (2002). . Apoptosis-inducing factor (AIF): a novel caspase-independent death effector released from mitochondria. *Biochimie*, **84**: 215-222.
- CHAN, W.H., WU, C.C., YU, J.S. (2003). Curcumin inhibits UVirradiation-induced oxidative stress and apoptotic biochemical changes in human epidermoid carcinoma A431 cells. *J Cell Biochem*, **90**: 327 –338.
- CHAN, W.H., WU, H.J.(2004). Anti-apoptotic effects of curcumin on photosensitized human epidermal carcinoma A431 cells. *J. Cell. Biochem*, **92**: 200 –212.
- CHAO D.T., KORSMEYER S.J. (1998). BCL-2 family: regulators of cell death. *Annu Rev Immunol*, **16**:395-419.
- CHEN, T., SAHIN, A., ALDAZ, C.M., (1996).Deletion map of chromosome 16q in ductal carcinoma in situ of the breast: Refining a putative tumour supressor gene region. *Cancer Res*, **56**: 5605-5609.
- CHENG, A.L., HSU, C.H., LIN, J.K., HSU, M.M., HO, Y.F., SHEN, T.S., KO, J.Y., LIN, J.T., LIN, B.R., MING-SHIANG, W., YU, H.S., JEE, S.H., CHEN, G.S., CHEN, T.M., CHEN, C.A., LAI, M.K., PU, Y.S., PAN, M.H., WANG, Y.J., TSAI, C.C., HSIEH, CY. (2001). Phase I clinical trial of curcumin, a chemopreventive agent, in patients with high-risk or pre-malignant lesions. *Anticancer Res*, **21**: 2895-2900.
- CHIARUGI, A., MOSKOWITZ, M.A. (2002). PARP-1 - a perpetrator of apoptotic cell death? *Science*, **297**: 200-201.
- CLARKE, P.G. (1990). Developmental cell death: morphological diversity and multiple mechanisms. *Anat Embryol*, **181**(3):195-213.
- CHOU, J.J., LI, H., SALVESEN, G.S., YUAN, J., WAGNER, G. (1999). Solution structure of BID, an intracellular amplifier of apoptotic signalling. *Cell*, **96** (5):615-24
- CLETON-JANSEN A.M., CALLEN, D.F., SESHADRI, R., GOLDUP, S., MCCALLUM, B., CRAWFORD, J., POWELL, J.A., SETTASATIAN, C., VAN BEERENDONK, H., MOERLAND, E.W., SMIT, V.T., HARRIS, W.H., MILLIS,

- R., MORGAN, N.V., BARNES, D., MATHEW, C.G., CORNELISSE, C.J. (2001). Loss of heterozygosity mapping at chromosome arm 16q in 712 breast tumors reveals factors that influence delineation of candidate regions. *Cancer Res*, **61**: 1171-1177.
- CODOGNO, P., MEIJER, A.J. (2005). Autophagy and signalling: their role in cell survival and cell death. *Cell Death Differ* **12** (2):1509-18.
- DANIAL, N.N., KORSEMEYER, S.J. (2004). Cell death: Critical control points. *Cell*, **116**: 205-219.
- DE DUVE, C. (1996). The birth of complex cells. *Sci Am*, April 1996.
- DENECKER, G., VERCAMMEN, D., STEEMANS, M., VANDEN BERGHE, T., BROUCKAERT, G., VAN LOO, G., ZHIVOTOVSKY, B., FIERS, W., GROOTEN, J., DECLERCQ, W., VANDENABEELE, P. (2001). Death receptor-induced apoptotic and necrotic cell death: Differential role of caspases and mitochondria. *Cell Death Differ*, **8** (8): 829-840.
- DESAGHER, S., OSEN-SAND, A., NICHOLS, A., ESKES, R., MONTESSUIT, S., LAUPER, S., MAUNDRELL, K., ANTONSSON, B., MARTINOU, J.C. (1999). Bid-induced conformational change of Bax is responsible for mitochondrial cytochrome c release during apoptosis. *J Cell Biol*, **144** (5):891-901.
- DEVERAUX QL, LEO E, STENNICKE HR, WELSH K, SALVESEN GS, REED JC. (1999). Cleavage of human inhibitor of apoptosis protein XIAP results in fragments with distinct specificities for caspases. *Embo J*, **18** (19):5242-51.
- DEVEREAUX, Q. L., TAKAHASHI R., SALVESEN G.S., REED J.C. (1997). X-linked IAP is a direct inhibitor of cell-death proteases. *Nature*, **388** (6639): 300-304.
- DYALL, S.D., BROWN, M.T., JOHNSON, P.J. (2004). Ancient invasions: From endosymbionts to organelles. *Science*, **304**: 253-257.
- EDINGER A.L., THOMPSON, C.B. (2003). Defective autophagy leads to cancer. *Cancer Cell*, December 2003: 422-424.
- EDINGER, A.L., THOMPSON, C.B. (2004). Death by design: apoptosis, necrosis and autophagy. *Current Opinion In Cell Biology*, **16**: 663-669.
- ELO, J.P., HARKONEN, P., KYLLONEN, A.P., LUKKARINEN, O., POUTANEN, M., VIHKO, R., VIHKO, P. (1997). Loss of heterozygosity at 16q24.1-q24.2 is significantly associated with metastatic and aggressive behavior of prostate cancer. *Cancer Res*, **57**: 3356-3359.
- ENARI, M., SAKAHIRA, H., YOKOYAMA, H., OKAWA, K., IWAMATSU, A., NAGATA, S. (1998). A caspase-activated DNase that degrades DNA during apoptosis, and its inhibitor ICAD. *Nature*, **391**: 43-50.

- FADOK, V.A., VOELKER, D.R., CAMPBELL, P.A., COHEN, J.J., BRATTON, D.L., HENSON, P.M. (1992). Exposure of phosphatidylserine on the surface of apoptotic lymphocytes triggers specific recognition and removal by macrophages. *J Immunol*, **148** (7): 2207-2216.
- FANG, J., *et al.* (2005). Thioredoxin reductase is irreversibly modified by Curcumin: A novel molecular mechanism for its anti-cancer activity. *Biol Chem*, **280**: 25284-25290.
- FENG, Z., ZHANG, H., LEVINE, A.J., JIN, S. (2005). The coordinate regulation of the p53 and mTOR pathways in cells. *Proc Natl Acad Sci USA*, **102**: 8204-8209.
- FESTJENS, N., VANDEB BERGHE, T., VANDENABEELE, P. (2006). Necrosis, a well orchestrated form of cell demise: signalling cascades, important mediators and concomitant immune response. *Biochim Biophys Acta*, **1757(9-10)** :1371-87.
- FURTH, P.A. (1999). Apoptosis and the development of breast cancer. In: Bowcock, a.m. Breast cancer: Molecular genetics, pathogenesis, and therapeutics. New Jersey: Humana Press. pp. 171-180.
- GARCEA, G., *et al.* (2005). Consumption of the putative chemopreventive agent Curcumin by cancer patients: Assessment of Curcumin levels in the colorectum and their pharmacodynamic consequences. *Cancer Epidemiol Biomarkers Prev*, **14**: 120-125.
- GARG, A.K., *et al.*(2005). Chemosensitization and radiosensitization of tumours by plant polyphenols. *Antioxid Redox Signal*, **7**: 1630-1647.
- GERMAIN, M., AFFAR, E-B., D'AMOURS, D., DIXIT, V.M., SALVESEN, G.S., POIRIER, G.G. (1999). Cleavage of automodified poly(ADP-ribose) polymerase during apoptosis. *J Biol Chem*, **274** (40): 28379-28384.
- GOMEZ, L.A., ALEKSEEV, A.E., ALEKSANDROVA, L.A., BRADY, P.A., TERZIC. (1997). Use of the MTT Assay in Adult Ventricular Cardiomyocytes to Assess Viability: Effects of Adenosine and Potassium on Cellular Survival. *J Mol Cell Cardiol*, **29 (4)**:1255-1266.
- GORMAN, A. J., MCCARTHY, J., FINUCANE, D., REVILLE, W., COTTER, T. (1994). Morphological assessment of apoptosis. In: Techniques in apoptosis, a user's guide. Cotter, T.G., Martin, S.J. Portland Press, New York. pp. 1-20.
- GOZUACIK, D., KIMCHI, A. (2004). Autophagy as a cell death and tumour suppressor mechanism. *Oncogene*, **23**: 2891-2906.
- GRANGE, J.M., STANFORD, J.L., STANFORD, A.C. (2002). Campbell De Morgan's 'Observations on cancer', and their relevance today. *J R Soc Med*, **95**: 296-299.

- HA, H.C., SNYDER, S.H. (1999). Poly(ADP-ribose) polymerase as a mediator of necrotic cell death by ATP depletion. *Proc Natl Acad Sci USA*, **96**: 13987-13982.
- HA, H.C., SNYDER, S.H., (2000). Poly(ADP-ribose) polymerase-1 in the nervous system. *Neurobiol Dis*, **7**: 225-239.
- HERR, I., DEBATIN, K-M. (2001). Cellular stress response in apoptosis in cancer therapy. *Blood*, **98**: 2603-2614.
- HOCKENBERY, D., NUÑEZ, G., MILLIMAN, C., SCHREIBER, R.D., KORSMEYER, S.J. (1990). Bcl-2 is an inner mitochondrial membrane protein that blocks programmed cell death. *Nature*, **348** (6299): 334-336.
- HOLLER, N., ZARU, R., MICHEAU, O., THOME, M., ATTINGER, A., VALITUTTI, S., BODMER, J.L., SCHNEIDER, P., SEED, B., TSCHOPP, J. (2000). Fas triggers an alternative, caspase-8-independent cell death pathway using the kinase RIP as effector molecule. *Nat Immunol*, **1**: 489-495.
- HOTZ, M.R., TRAGANOS, F., DARZYNKIEWICZ. (1992). Changes in nuclear chromatin related to apoptosis or necrosis induced by the DNA topoisomerase II inhibitor fostriecin in MOLT-4 and HL-60 cells are revealed by altered DNA sensitivity to denaturation. *Exp Cell Res*, **201**: 184-191.
- HUSSAIN, A.R., AL-RASHEED, M., MANOGARAN, P.S., AL-HUSSEIN, K. A., *et al.* (2006). Curcumin induces apoptosis via inhibition of PI3'-kinase/AKT pathway in acute T cell leukemias. *Apoptosis*, **11**: 245 –254.
- IRESON, C.R., *et al.* (2002). Metabolism of the cancer chemopreventive agent Curcumin in human and rat intestine. *Cancer Epidemiol Biomarkers Prev*, **11**: 105-111.
- JAATTELA, M., TSCHOPP, J. (2003). caspase-independent cell death in T lymphocytes. *Nat Immunol*, **4**: 416-423.
- JANICKE, R.U., SPRENGART, M.L., WAIT, M.R., PORTER, A.G. (1998). Caspase-3 is required for DNA fragmentation and morphological changes associated with apoptosis. (1998). *J Biol Chem*, **273**: 9357-9360.
- JEMAL, A., SIEGEL, R., WARD, E., HAO, Y., XU, J., MURRAY, T., THUN, M.J. (2008). Cancer statistics, 2008. *CA Cancer J Clin*, **58**: 71-96.
- JIN, S. (2006). Autophagy, mitochondrial quality control, and oncogenesis. *Autophagy*, **2**(2): 80-84.
- KAMANGAR, F., DORES, G.M., ANDERSON, W.F. (2006). Patterns of cancer incidence, mortality and prevalence across five continents: defining priorities to reduce cancer disparities in different geographic regions of the world. *J Clin Oncol*, **24**: 2173-2150.

- KARMAKAR, S., BANIK, N.L., PATEL, S.J., RAY, S.K. (2006). Curcumin activated both receptor-mediated and mitochondria-mediated proteolytic pathways for apoptosis in human glioblastoma T98G cells. *Neurosci Lett*, **407**: 53–58.
- KARMAKAR, S., BANIK, N.L., RAY, S.K. (2007). Curcumin suppressed anti-apoptotic signals and activated cysteine proteases for apoptosis in human malignant glioblastoma U87MG cells. *Neurochem Res*, **32**: 2103–2113.
- KARPOZILOS, A., PAVLIDIS, N. (2004). The treatment of cancer in Greek antiquity. *Eur J Cancer*, **40**: 2033-2040.
- KASIBHATLA, S., TSENG, B. (2003). Why target apoptosis in cancer treatment? *Mol Canc Ther*, **2**: 573-580.
- KATZ, R.K., JOHNSON, T.S., WILLIAMSON, K.D. (1985). Comparison of cytologic and acridine orange flow cytometric detection of malignant cells in human body cavity fluids. *Anal Quant Cytol*, **7**: 227-235.
- KERR, R.O., CARDAMONE, J., DALMASSO, A.P., KAPLAN, M.E. (1972). Two mechanisms of erythrocyte destruction in penicillin-induced hemolytic anemia. *N Engl J Med*, **287**(26): 1322-1325.
- KHAR, A., ALI, A.M., PARDHASARADHI, B.V., BEGUM, Z., ANJUM, R. (1999). Antitumor activity of curcumin is mediated through the induction of apoptosis in AK-5 tumor cells. *FEBS Lett*, **445**: 165–168.
- KOMATSU, M., WAGURI, S., UENO, T., IWATA, J., MURATA, S., TANIDA, I., EZAKI, J., MIZUSHIMA, N., OHSUMI, Y., UCHIYAMA, Y., KOMINAMI, E., TANAKA, K., CHIBA, T. (2005). Impairment of starvation -induced and constitutive autophagy in *Atg-7* deficient mice. *J Cell Biol*, **169**: 425-434.
- KROEMER, G., GALLUZZI, L., VANDENABEELE, P., ABRAMS, J., ALNEMRI, E.S., BAEHRECKE, E.H., BLAGOSKLONNY, M.V., EL-DEIRY, W.S., GOLSTEIN, P., GREEN, D.R., HENGARTNER, M., KNIGHT, R.A., KUMAR, S., LIPTON, S.A., MALORNI, W., NUÑEZ, G., PETER, M.E., TSCHOPP, J., YUAN, J., PIACENTINI, M., ZHIVOTOVSKY, B., MELINO, G. (2009). Nomenclature Committee on Cell Death 2009. Classification of cell death: recommendations of the Nomenclature Committee on Cell Death 2009. *Cell Death Differ*, **16**(1):3-11.
- KROEMER, G., REED, J.C. (2000). Mitochondrial control of cell death. *Nat Med*, **6** (5): 513-519.
- KRYSKO, D.V., VANDEN BERGHE.T., D'HERDE, K., VANDENABEELE P. (2008). Apoptosis and necrosis: Detection, discrimination and phagocytosis. *Methods*, **44** (3): 205-221.

- KUNAPULI, S., ROSANIO, S., SCHWARZ, E.R. (2006). "How do cardiomyocytes die?" apoptosis and autophagic cell death in cardiac myocytes. *J Card Fail*, **12(5)**:381-91.
- KUROKAWA, H., KAZUTO, N., FUKUMOTO, H., TOMONARI, A., SUZUKI, T., SAIJO, N. (1999). Alteration of caspase-3 (CPP32/Yama/apopain) in wild-type MCF-7 breast cancer cells. *Oncology Rep*, **6**: 33-37.
- LI, H., ZHU, H., XU, C.J., YUAN, J. (1998). Cleavage of BID by caspase 8 mediates the mitochondrial damage in the Fas pathway of apoptosis. *Cell*, **94(4)**:491-501.
- LI, J., YEN, C., LIAW, D., PODSYPANINA, K., BOSE, S., WANG, S.I., PUC, J., MILIAREISIS, C., RODGERS, L., MCCOMBIE, R., BINGER, S.H., GIOVANELLA, B.C., ITTMAN, M., TYCKO, B., HIBSHOOSH, H., WIGGLER, M.H., PARSONS, R. (1997). *PTEN*, a putative protein tyrosine phosphatase gene mutated in human brain, breast and prostate cancer. *Science*, **257**:1943-1947.
- LIANG, X., H., JACKSON, S., SEAMAN, M., BROWN, K., KEMPKES, B., HIBSHOOSH, H., LEVINE, B. (1999). Induction of autophagy and inhibition of tumorigenesis by *beclin 1*. *Nature*, **402**: 762-776.
- LIANG, Y., YAN, C., SCHOR, N.F. (2001). Apoptosis in the absence of caspase-3. *Oncogene*, **20**: 6570-6578).
- LOCKSHIN, R.A., ZAKERI, Z. (2001). Programmed cell death and apoptosis: origins of the theory. *Nature Reviews*, **2**: 545-550.
- LOCKSHIN, R.A., ZAKERI, Z. (2004). Caspase-independent cell death? *Oncogene*, **23**: 2766-2773.
- LUO, X., BUDIARDJO, I., ZOU, H., SLAUGHTER, C., WANG, X. (1998). Bid, a Bcl2 interacting protein, mediates cytochrome c release from mitochondria in response to activation of cell surface death receptors. *Cell*, **94(4)**:481-90.
- MAIURI, M., ZALCKVAR, E., KIMCHI, A., KROEMER, G. (2007). Self-eating and self-killing: crosstalk between autophagy and apoptosis. *Nat Rev Mol Cell Biol*, **8 (9)**: 741-52.
- MAJNO, G., JORIS, I. (1995). Apoptosis, oncosis and necrosis. An overview of cell death. *Am J Pathol*, **146 (1)**: 3-15.
- MEIJER, A.J., CODOGNO, P. (2004). Regulation and role of autophagy in mammalian cells. *Int J Biochem Cell Biol*, **36 (12)**:2445-62
- MIZUSHIMA, N., YOSHIMORI, T. (2007). How to interpret LC3 immunoblotting. *Autophagy*, **3 (6)**: 542-545.

- MCDONNELL, J.M., FUSHMAN, D., MILLIMAN, C.L., KORSMEYER, S.J., COWBURN, D. (1999). Solution structure of the proapoptotic molecule BID: a structural basis for apoptotic agonists and antagonists. *Cell*, **96 (5)**:625-34.
- MUCHMORE S.W., SATTLER M., LIANG H., MEADOWS R.P., HARLAN J.E., YOON H.S., NETTESHEIM D., CHANG B.S., THOMPSON C.B., WONG S.L., FESIK, S.W. (1996). X-ray and NMR structure of human Bcl-xL, an inhibitor of programmed cell death. *Nature*, **381 (6580)**:335-41.
- NIV, H., GUTMAN, O., HENIS, Y.I., KLOOG, Y. (1999). Membrane interactions of a constitutively active GFP-Ki-Ras 4B and their role in signalling. Evidence from lateral mobility studies. *J Biol Chem*, **274**:1606–13.
- NOTARBARTOLO, M., POMA, P., PERRI, D., DUSONCHET, L., *ET AL.* (2005). Antitumor effects of curcumin, alone or in combination with cisplatin or doxorubicin, on human hepatic cancer cells. Analysis of their possible relationship to changes in NF-kB activation levels and in IAP gene expression. *Cancer Lett*, **224**: 53–65.
- OKADA M., ADACHI S., IMAI T., WATANABE K., TOYOKUNI S.Y., UENO M., ZERVOS A.S., KROEMER G., NAKAHATA T. (2004). A novel mechanism for imatinib mesylate-induced cell death of BCR-ABL-positive human leukemic cells: caspase-independent, necrosis-like programmed cell death mediated by serine protease activity. *Blood*, **103(6)**: 2299-307.
- OLTVAI, Z.N., MILLIMAN, C.L., KORSMEYER, S.J. (1993). Bcl-2 heterodimerizes in vivo with a conserved homolog, Bax, that accelerates programmed cell death. *Cell*, **74(4)**:609-19
- ORMEROD, M.G., COLLINS, M.K.L., RODRIGUEZ-TARDUCHY, G., ROBERTSON, D. (1992). Apoptosis in interleukin-3 dependent haemopoietic cells: quantification by two flow cytometric methods. *J Immunol Meth*, **153**: 57-65.
- PARKIN, D.M., BRAY, F., FERLAY, J., PISANI, P. (2002). Global cancer statistics 2002. *CA Cancer J Clin*, **55**: 74-108.
- PEROU, C.M., SØRLIE, T.; EISEN, M.B., VAN DE RIJN, M., JEFFREY, S.S., REES, CA., POLLACK, J.R., ROSS, D.T., JOHNSEN, H., AKSLEN, L.A., FLUGE, Ø., PERGAMENSCHIKOV, A.; WILLIAMS, C., ZHU, S.X., LØNNING, P.E., BØRRESEN-DALE, A-L., BROWN, P.O., BOTSTEIN, D. (2000). Molecular portraits of human breast tumours. *Nature*, **406**: 747-752.
- PETROS, A.M., MEDEK, A., NETTESHEIM, D.G., KIM, D.H., YOON, H.S., SWIFT, K., MATAYOSHI, E.D., OLTERS DORF, T., FESIK, S.W. (2001). Solution structure of the antiapoptotic protein bcl-2. *Proc Natl Acad Sci U S A*, **98(6)**:3012- 3017
- POLYAK, K. (2007). Breast cancer: Origins and evolution. *J Clin Invest*, **117**: 3155-3163.

- POULAKI, V., MITSIADES C.S., MITSIADES, N. (2001). The role of fas and fasL as mediators of anticancer chemotherapy. *Drug resist Updat*, **4**: 233-242.
- REED, J.,C. (1996).Mechanisms of Bcl-2 family protein function and dysfunction in health and disease. *Behring Inst Mitt*, **97**:72-100.
- ROY N., DEVERAUX Q.L., TAKAHASHI R., SALVESEN G.S., REED J.C. (1997). The c-IAP-1 and c-IAP-2 proteins are direct inhibitors of specific caspases. *Embo J* **16 (23)**:6914-25.
- RUBINSZTEIN, D.C., DIFIGLIA, M., HEINTZ, N., NIXON, R.A., QIN, Z.H., RAVIKUMAR, B., STEFANIS, L., TOLKOVSKY, A. (2005). Autophagy and its possible roles in nervous system diseases, damage, and repair. *Autophagy*, **1(1)**: 11-22.
- SATTLER, M., LIANG, H., NETTESHEIM, D., MEADOWS, R.P., HARLAN, J.E., EBERSTADT, M., YOON, H.S., SHUKER, S.B., CHANG, B.S., MINN, A.J., THOMPSON, C.B., FESIK, S.W. (1997). Structure of Bcl-xL-Bak peptide complex: recognition between regulators of apoptosis. *Science*, **275 (5302)**:983-6
- SCHMID I., UITTENBOGAART, C.U., GIORGI, J.V. (1994). A sensitive method for measuring apoptosis and cell surface phenotype in human thymocytes by flow cytometry. *Cytometry*, **15**: 12-20.
- SCHMID, D., MUENZ, C. (2007). Innate and adaptive immunity through autophagy. *Immunity*, **27(1)**: 11-21.
- SCHWEICHEL, J.U., MERKER, H.J. (1973). The morphology of various types of cell death in prenatal tissues. *Teratology*, **7(3)**:253-66.
- SHALL, S., DE MURCIA, G. (2000). Poly(ADP-ribose) polymerase-1: what have we learned from the deficient mouse model? *Mutation Res*, **460**: 1-15.
- SHISHODIA, S., AMIN, H.M., LAI, R., AGGARWAL, B.B. (2005). Curcumin (diferuloylmethane) inhibits constitutive NF-kappaB activation, induces G1/S arrest, suppresses proliferation, and induces apoptosis in mantle cell lymphoma. *Biochem Pharmacol*, **70**: 700–713.
- SHOBA, G., JOY, D., JOSEPH, T., MAJEED, M., RAJENDRAN, R., SRINIVAS, P.S. (1998). Influence of piperine on the pharmacokinetics of curcumin in animals and human volunteers. *Planta Med*, **64**: 353–356.
- SIEMANKOWSKI, L.M., MORREALE, M.M., BRIEHL, M.M. (1999). Antioxidant defenses in TNF-related MCF-7 cells: Selective increase in MnSOD. *Free Radic Biol Med*, **26**: 919-924.

- SIWAK, D.R., SHISHODIA, S., AGGARWAL, B.B., KURZROCK, R. (2005). Curcumin-induced antiproliferative and proapoptotic effects in melanoma cells are associated with suppression of I κ B kinase and nuclear factor κ B activity and are independent of the B-Raf/mitogen-activated/extracellular signal-regulated protein kinase pathway and the Akt pathway. *Cancer*, **104(4)**:879-90.
- SLEE, E.A., KEOGH, S.A., MARTIN, S.J. (2000). Cleavage of BID during cytotoxic drug and UV radiation-induced apoptosis occurs downstream of the point of Bcl-2 action and is catalysed by caspase-3: a potential feedback loop for amplification of apoptosis-associated mitochondrial cytochrome c release. *Cell Death Differ*, **7(6)**:556-65.
- SONG, G., MAO, Y.B., CAI, Q.F., YAO, L.M., ET AL. (2005). Curcumin induces human HT-29 colon adenocarcinoma cell apoptosis by activating p53 and regulating apoptosis-related protein expression. *Braz J Med Biol Res*, **38**: 1791 –1798.
- SORLIE, T., PEROU, C.M., TIBSHIRANIE, R., AASF, T., GEISLERG, S., JOHNSEN, H., HASTIE, T., EISEN, B.M., VAN DE RIJN, M., JEFFREY, S.S., THORSENK, T., QUISTL, H., MATESE, J.C., BROWN, P.O., BOTSTEIN, D., LØNNING, P.E., BØRRESEN-DALE, A-L. (2001). Gene expression patterns of breast carcinomas distinguish tumor subclasses with clinical implications. *Proc Natl Acad Sci USA*, **98**: 10869-10874.
- SUZUKI, Y., IMAI, Y., NAKAYAMA, H., TAKAHASHI, K., TAKIO, K., TAKAHASHI, R. (2001). A serine protease, HtrA2, is released from the mitochondria and interacts with XIAP, inducing cell death. *Mol Cell*, **8**: 613-621.
- SYING-AI, C., et al. (2004). Effect of Curcumin on normal and tumour cells: Role of glutathione and bcl-2. *Mol Cancer Ther*, **3**: 1101-1108.
- SUZUKI M., YOULE R.J., TJANDRA N. (2000). Structure of Bax: coregulation of dimer formation and intracellular localization. *Cell*, **103 (4)**:645-54.
- TANIDA, I., UENO, T., KOMINAMI, E. (2004). Human light chain 3/MAP1LC3B is cleaved at its carboxyl-terminal Met121 to expose Gly120 for lipidation and targeting to autophagosomal membranes. *J Biol Chem*, **297 (46)**: 44704-44710.
- TSUKADA, M., OHSUMI, Y. (1993). Isolation and characterization of autophagy-defective mutants of *Saccharomyces cerevisiae*. *FEBS Lett*, **333**: 169-174.
- TSVETKOV, P., ASHER, G., REISS, V., SHAUL, Y., et al. (2005). Inhibition of NAD(P)H:quinone oxidoreductase 1 activity and induction of p53 degradation by the natural phenolic compound curcumin. *Proc Natl Acad Sci USA*, **102**: 5535–

- VANDEN BERGHE, T., DECLERCQ, W., VANDENABEELE, P. (2007). NADPH oxidases: new players in TNF-induced necrotic cell death. *Moll Cell*, **26 (6)**: 769-771.
- VAN LOO, G., DEMOL, H., VAN GURP, M., HOORELBEKE, B., SCHOTTE, P., BEYART, R., ZHIVOTOVSKY, B., GEVAERT, K., DECLERCQ, W., VANDEKERCKHOVE, J., VANDENABEELE, P. (2002). A matrix-assisted laser desorption ionization post-source decay (MALDI-PSD) analysis of proteins released from isolated liver mitochondria treated with recombinant truncated Bid. *Cell Death Differ*, **9 (3)**: 301-308.
- VAUX, D.L., CORY, S., ADAMS, J.M. (1988). Bcl-2 gene promotes haemopoietic cell survival and cooperates with c-myc to immortalize pre-B cells. *Nature*, **335 (6189)**:440-442.
- VERCAMMEN, D., BEYAERT, R., DENECKER, G., GOOSSENS, V., VAN LOO, G., DECLERCQ, W., GROOTEN, J., FIERS, W., VANDENABEELE, P. (1998). Inhibition of caspases increases the sensitivity of L929 cells to necrosis mediated by tumour necrosis factor. *J Exp Med*, **187**: 1477-1485.
- VINDELOV, L.L., CHRISTENSEN, I.J., NISSEN, N.I. (1983). A detergent-trypsin method for the preparation of nuclei for flow-cytometric DNA analysis. *Cytometry*, **3**: 323-327.
- WOLF, B.B., SCHULER, M., ECHEVERRI, F., GREEN, D.R. (1999). Caspase-3 is the primary activator of apoptotic DNA fragmentation via DNA fragmentation factor-45/inhibitor of caspase-activated DNase inactivation. *J Biol Chem*, **274**: 30651-30656.
- YANG, E., ZHA, J., JOCKEL, J., BOISE, L.H., THOMPSON, C.B., KORSMEYER, S.J. (1995). Bad, a heterodimeric partner for Bcl-XL and Bcl-2, displaces Bax and promotes cell death. *Cell*, **80 (2)**:285-91.
- YEH, C. H., CHEN, T. P., WU, Y. C., LIN, Y. M., JING LIN, P., YEH, C.H., LIN, Y.M., WU, Y.C., LIN, P.J. (2005). Inhibition of NFkappa B activation can attenuate ischemia/reperfusion induced contractility impairment via decreasing cardiomyocytic proinflammatory gene up-regulation and matrix metalloproteinase expression. *J Cardiovasc Pharmacol*, **45**: 301–309.
- YU, Q., X., BHAGAT, B., FURUYA, N., HIBSHOOSH, H., TROXEL, A., ROSEN, J., ESKELINEN, E.L., MIZUSHIMA, N., OHSUMI, Y., CATTORETTI, G., LEVINE, B. (2003). Promotion of tumorigenesis by heterozygous disruption of the *beclin 1* autophagy gene. *J Clin Invest*, **112**: 1809-1820.
- YU, S.W., WANG, H., POITRAS, M.F., COOMBS, C., BOWERS, W.J., FEDEROFF, H.J., POIRIER, G.G., DAWSON, T.M., DAWSON, V.L.. (2002). Mediation of poly(ADP-ribose) polymerase-1-dependent cell death by apoptosis-inducing factor. *Science*, **297**: 259-263.

- YUAN, J., YANKNER, B.A. (2000). Apoptosis in the nervous system. *Nature*, **407**: 802-809.
- ZHA, H., AIMÉ-SEMPÉ, C., SATO, T., REED, J.C. (1996). Proapoptotic protein Bax heterodimerizes with Bcl-2 and homodimerizes with Bax via a novel domain (BH3) distinct from BH1 and BH2. *J Biol Chem*, **271 (13)**:7440-7444.
- ZONG, W.X., DITSWORTH, D., BAUER, D.E., WANG, Z.Q., THOMPSON, C.B. (2004). Alkylating DNA damage stimulates a regulated form of necrotic cell death. *Genes Dev*, **18**: 1272-1282.

Addendum 1: Cell culture consumables

1.1 Growth medium

MCF-7:

- ▶ Dulbecco's Modified Eagle's Medium (SIGMA)
- ▶ 5% Foetal Bovine Serum (Gibco)
- ▶ 1% 2 mM L-Glutamine (SIGMA)

MCF-12A:

- ▶ 50% Dulbecco's Modified Eagle's Medium (SIGMA)
 - ▶ 50% Ham's F12 Medium (SIGMA)
 - ▶ 5% Foetal Bovine Serum (Gibco)
 - ▶ 20 ng/ml Human recombinant Epidermal Growth Factor (Invitrogen)
 - ▶ 500 ng/ml Hydrocortisone (SIGMA)
 - ▶ 2.4 µl/ml Insulin (Humalog)
-

1.2 General reagents and plastic ware

<i>Item</i>	<i>Manufacturer</i>
▶ 12-Well Plates	Nunc Lab-Tek
▶ 22µM Syringe Filters	Whatman
▶ 6-Well Plates	Nunc Lab-Tek
▶ 8-Chamber Dishes	Nunc Lab-Tek
▶ Bovine Serum Albumen (BSA)	SIGMA
▶ Cell scrapers	Nalge Nunc International
▶ Centrifuge Tubes	BD Falcon
▶ Curcumin	SIGMA
▶ DMEM	SIGMA
▶ Dulbecco's Phosphate Buffered Saline	Prepared by Laboratory Technician
▶ Eppendorf Tubes	Greiner bio-one
▶ Ethyl Alcohol (CH ₃ CH ₂ OH)	Illovo
▶ FBS	Gibco
▶ L-Glutamine	SIGMA
▶ Pipette Tips	Quality Scientific Plastics
▶ Serological Pipettes	LP Italiana SP, Sterilin
▶ Syringes	Surgi Plus
▶ Tissue Culture Flasks	Greiner Bio-One
▶ Trypsin-EDTA	SIGMA

Addendum 2: Reagents and solutions used for immunocytochemistry

2.1. 1% Paraformaldehyde (non permeabilizing cell fixative)

Ingredients (for 100 ml):

- i. Paraformaldehyde
- ii. dH₂O
- iii. 1 M NaOH
- iv. PBS

Method:

- ▶ *Add 5 ml dH₂O to 1 g Paraformaldehyde*
 - ▶ *Add 10 drops of 1M NaOH*
 - ▶ *Heat to 80°C in water bath; incubate 2-3 minutes at 80°C while shaking*
 - ▶ *When Paraformaldehyde has dissolved, add 95 ml PBS*
-

2.2 Hoechst Staining Solution

Ingredients (Stock Solution):

- i. Hoechst 3334
- ii. dimethyl sulfoxide (DMSO)

Method:

- ▶ *Add 2 mg/ml Hoechst 3334 to DMSO; mix; store at 4°C*

Ingredients (Working Solution):

- i. Hoechst 3334 Stock Solution
- ii. PBS

Method:

- ▶ *Add 1.4 ml of Hoechst 3334 Stock Solution to 1 ml PBS*
 - ▶ *Mix by tapping with finger*
 - ▶ *Use supernatant only*
-
-

2.3 Acridine Orange Staining Solution

Ingredients:

- i. 6 µg/ml Acridine Orange
- ii. 0.1 M Citric Acid

Method:

- ▶ *Add 19.21 g Citric Acid to 1 L dH₂O; stir*

- iii. 0.2 M Na₂HPO₄ pH 2.6

Method:

- ▶ *Add 14.19 g Na₂HPO₄ to 500 ml dH₂O; stir*

Method:

- ▶ *Add 6 µg/ml Acridine Orange to 90 ml of 0.1 M Citric Acid*
 - ▶ *Add 10 ml of 0.2 M Na₂HPO₄ pH 2.6; mix; protect from light; store at 4°C*
-
-

Addendum 3: Solutions and reagents used for protein detection

3.1 Radioimmunoprecipitation (RIPA) buffer (100 ml)

Ingredients:

i. 50 mM Tris-HCl pH 7.4

a. Method:

Add 790 mg Tris to 75 ml dH₂O

Add 900 mg HCl; stir

Adjust pH to 7.4 using HCl

ii. 10% NP-40

Method:

Add 1 ml NP-40 to 9 ml dH₂O; stir

iii. 10% Na-deoxycholate

Method:

Add 0.125 g Na- deoxycholate to 5 ml dH₂O; protect from light; stir

iv. 100 mM EDTA pH 7.4

Method:

Add 3.722 g EDTA to 100 ml dH₂O; stir

Adjust pH to 7.4

v. 200 mM Phenylmethylsulfonyl fluoride (PMSF)

Method:

Add 0.034g PMSF to 1 ml Isopropanol; mix; store at RT

vi. 1 mg/ml Leupeptin

a. Method:

Add 1 mg Leupeptin to 1 ml dH₂O; mix; store at -20°C

vii. 5 mg/ml SBT1

Method:

Add 5 mg SBT1 to 1 ml dH₂O; mix; store at -20°C

viii. 1 M Benzamidine (SIGMA)

a. Method:

Add 0.05g Benzamidine to 1ml Abs MeOH; mix; store at -20°C

ix. 200 mM Activated Na₃VO₄

a. Method:

Add ; mix; store at -20°C

x. 200 mM Sodium Fluoride (NaF)

Add 0.0083 g NaF to 1 ml dH₂O; mix; store at -20°C

xi. Triton X-100

xii. dH₂O

Method (on ice)

- ▶ *Thaw protease and phosphatase inhibitors on ice*
 - ▶ *Add 10ml of 10% NP-40 to prepared 50 mM Tris-HCl*
 - ▶ *Add 2.5 ml of 10% Na-deoxycholate; stir*
 - ▶ *Add 1 ml of 100 mM EDTA pH 7.4*

Add following protease inhibitors, while stirring, on ice:

- ▶ *500 μ l of 200 mM PMSF*
- ▶ *100 μ l of 1 mg/ml Leupeptin*
- ▶ *800 μ l of 5 mg/ml SBT1*
- ▶ *100 μ l of 1 M Benzamidine*

Add following phosphatase inhibitors

- ▶ *500 μ l of 200 mM Activated Na_3VO_4*
 - ▶ *500 μ l of 200 mM NaF*
 - ▶ *Add 1 ml of Triton X-100*
 - ▶ *Make up to 100 ml with dH₂O*
 - ▶ *Make 1 ml aliquots and store at -20°C*
-
-

3.2 Bradford Reagent (6 x concentrated)

Ingredients:

- i. Coomassie Brilliant Blue G
- ii. 95% EtOH
- iii. Phosphoric Acid
- iv. dH₂O

Method:

- ▶ *Dilute 500 mg Coomassie Brilliant Blue G in EtOH*
- ▶ *Add 500 ml Phosphoric Acid; mix thoroughly*
- ▶ *Make up to 1 L with dH₂O*
- ▶ *Filter; protect from light; store at 4°C*

Bradford Working Solution

Ingredients:

- i. Bradford Reagent (6 x concentrated)
- ii. dH₂O

Method:

- ▶ *Dilute 6 x stock 1:5 using dH₂O*
 - ▶ *Filter, using 2 filter papers simultaneously*
-

3.3 Laemmli Sample Buffer

Ingredients:

- i. 12.5 ml 0.5 M Tris-HCl pH 6.8
- ii. 7.5 g Glycerol
- iii. 5 ml β -mercaptoethanol
- iv. 0.2 g Bromophenol Blue
- v. 3.3 g SDS

Method:

- ▶ *Combine all ingredients; stir*
 - ▶ *Store at RT*
-

3.4. 10%, 1 mm SDS Separating Gel

Ingredients (sufficient for 4 gels):

- i. dH₂O
- ii. 1.5 M Tris-HCl pH 8.8

Method:

- ▶ Weigh off 181.17 g Tris
- ▶ Make up to 1 L using dH₂O; stir
- ▶ Adjust pH to 8.8 using HCl; store at 4 °C

- iii. 10% SDS

Method:

- ▶ Weigh off 100g SDS
- ▶ Make up to 1 L with dH₂O; stir; store at RT

- iv. 10% Ammonium persulphate (APS)

Method:

- ▶ Weigh off 0.1g APS
- ▶ Make up to 1 ml with dH₂O; vortex

- v. 40% Acrylamide

- vi. Temed

Method

- ▶ Add 10 ml of 1.5 M Tris-HCl pH 8.8 to 15.4 ml dH₂O
- ▶ Add 400 µl of 10% SDS
- ▶ Add 10 ml of 40% Acrylamide
- ▶ Add 200 µl of 10% APS; stir briefly
- ▶ Add 20 µl of Temed in fume hood; stir briefly

4%, 1 mm SDS Stacking Gel

Ingredients:

- i. dH₂O
- ii. 0.5 M Tris-HCl pH 6.8

Method:

- ▶ Weigh off 60.57 g Tris
- ▶ Make up to 1 L using dH₂O; stir
- ▶ Adjust pH to 6.8 using HCl; store at 4 °C

- iii. 10% SDS

Method:

- ▶ Weigh off 100g SDS

- ▶ *Make up to 1 L with dH₂O; stir; store at RT*

iv. 10% APS

Method:

- ▶ *Weigh off 0.1g APS*
- ▶ *Make up to 1 ml with dH₂O; vortex*

v. 40% Acrylamide

vi. Temed

Method:

- ▶ *Add 2500 ml of 0.5 M Tris-HCl pH 6.8 to 6100 ml dH₂O*
 - ▶ *Add 100 μ l of 10% SDS*
 - ▶ *Add 1 ml of 40% Acrylamide*
 - ▶ *Add 100 μ l of 10% APS; stir briefly*
 - ▶ *Add 10 μ l of Temed in fume hood; stir briefly*
-
-

3.5 Anode Buffer 1

Ingredients:

- i. Trizma® base (Tris)
- ii. dH₂O
- iii. Abs MeOH

Method:

- ▶ Add 18.2 g Tris to 380 ml H₂O; stir
- ▶ Adjust pH to 10.4
- ▶ Add 100 ml of Abs MeOH
- ▶ Make up to 500 ml with dH₂O, mix, store at 4°C

Anode Buffer 2

Ingredients:

- i. Tris
- ii. dH₂O
- iii. Abs MeOH

Method:

- ▶ Add 1.51g Tris to 380 ml H₂O; stir
- ▶ Adjust pH to 10.4
- ▶ Add 100 ml of Abs MeOH
- ▶ Make up to 500 ml with dH₂O, mix, store at 4°C

Cathode Buffer

Ingredients:

- i. Tris
- ii. 6- Aminohexanoic acid
- iii. dH₂O
- iv. Abs MeOH

Method:

- ▶ Add 1.51g Tris to 380 ml H₂O; stir
 - ▶ Add 2g. 6- Aminohexanoic acid; stir
 - ▶ Adjust pH to 9.4
 - ▶ Add 100 ml of Abs MeOH
 - ▶ Make up to 500 ml with dH₂O, mix, store at 4°C
-

3.6 Running Buffer (10x)

Ingredients (for 1 L):

- i. 30g Tris
- ii. 144g Glycine
- iii. 10g SDS
- iv. dH₂O

Method

- ▶ *Weigh off dry ingredients, add together*
 - ▶ *Make up to 1 L using dH₂O; stir*
 - ▶ *Adjust pH to 8.3; store at 4°C*
-
-

3.7 Tris-Buffered Saline (TBS)

Ingredients:

- v. 3g Tris
- vi. 8g NaCl
- vii. 0.2g KCl
- viii. dH₂O

Method

- ▶ *Weigh off dry ingredients, add together*
 - ▶ *Make up to 1 L using dH₂O; stir*
 - ▶ *Adjust pH to 7.4; store at 4°C*
-
-